Chemical Science

ROYAL SOCIETY OF CHEMISTRY

PERSPECTIVE

View Article Online
View Journal | View Issue

Cite this: *Chem. Sci.*, 2020, **11**, 12249

All publication charges for this article have been paid for by the Royal Society of Chemistry

Received 20th August 2020
Accepted 13th October 2020

DOI: 10.1039/d0sc04585c

rsc.li/chemical-science

Over one century after discovery: pyrylium salt chemistry emerging as a powerful approach for the construction of complex macrocycles and metallo-supramolecules

Yiming Li, [ab] Heng Wang[a] and Xiaopeng Li *[a]

Over one century after its discovery, pyrylium salt chemistry has been extensively applied in preparing light emitters, photocatalysts, and sensitizers. In most of these studies, pyrylium salts acted as versatile precursors for the preparation of small molecules (such as furan, pyridines, phosphines, pyridinium salts, thiopyryliums and betaine dyes) and poly(pyridinium salt)s. In recent decades, pyrylium salt chemistry has emerged as a powerful approach for constructing complex macrocycles and metallo-supramolecules. In this perspective, we attempt to summarize the representative efforts of synthesizing and self-assembling large, complex architectures using pyrylium salt chemistry. We believe that this perspective not only highlights the recent achievements in pyrylium salt chemistry, but also inspires us to revisit this chemistry to design and construct macrocycles and metallo-supramolecules with increasing complexity and desired function.

1. Introduction

Pyrylium salts are a type of six-membered cationic heterocycles with one positively charged oxygen atom. Compounds with pyrylium salts exhibit excellent absorption, fluorescence, and electron transfer properties, and thus have been widely applied as light emitters,[1] photocatalysts,[2] and sensitizers.[3–6] The first pyrylium salt with perchlorate as the counterion was reported in 1911 by Baeyer;[7] however, since the discovery of pyrylium salts, such salts have been underappreciated for about a half-century. Until 1960s, the importance of pyrylium salts has been realized as versatile precursors in a wide array of organic syntheses.[8–10] Due to their high reactivity towards various nucleophiles, pyrylium salts were widely employed for the convenient synthesis of diverse heterocyclic compounds.

Starting from 1980s,[11] the high reactive features of pyrylium salts were further utilized to synthesize viologen polymers with pyridinium salts in the backbones. Through the facile

[a]College of Chemistry and Environmental Engineering, Shenzhen University, Shenzhen 518055, China. E-mail: xiaopengli@szu.edu.cn
[b]Department of Chemistry, University of South Florida, Tampa, Florida 33620, USA

Yiming Li received his MS degree in chemistry at Central South University, China in 2016. Afterwards, he joined the group of Prof. Xiaopeng Li at the University of South Florida, and received his PhD degree in 2020. His research interests mainly focus on coordination-driven self-assembly and scanning tunneling microscopy.

Heng Wang received his BS and PhD in chemistry from Peking University in 2009 and 2015, respectively. After one year of postdoctoral training at Hokkaido University, he then worked with Prof. Xiaopeng Li at the University of South Florida from 2016 to 2020 as a postdoctoral associate. In 2020, he started to work as an Associate Professor in Shenzhen University, China. His major research interests focus on the self-assembly and hierarchical self-assembly of metallo-supramolecules, and seeking the novel application of supramolecular assemblies.

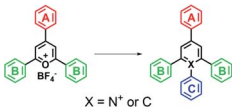

Fig. 1 Transformations of pyrylium salts to arenes or pyridinium salts.

polymerization process by condensation reactions between bis-pyrylium salts and primary diamines, a variety of cationic pyridinium polymers were synthesized and simply purified by precipitation and washing.[11,12] Benefiting from their positive charges on the backbones and the aromatic structures, such poly(pyridinium salt)s[13,14] have displayed magnificent features, such as electrochromism,[15,16] photochromism,[17] thermochromism,[18] liquid-crystalline[19,20] and sensitive DNA detectability,[21,22] thus, have attracted much attention in the fields of chemistry, physics and biology.

Compared with the well-documented study in small molecules and polymers based on pyrylium salt chemistry,[23,49] very few works were focused on utilizing this approach in constructing large, discrete molecules, perhaps because of the challenge on the molecular design and the lack of an efficient purification strategy for the charged species. During the past two decades, pyrylium salts have been employed by Höger and Müllen as a powerful tool for the preparation of discrete organic macrocycles with well-defined sizes, shapes and structures.[24–26] By utilizing the transformation of the functionalized 2,4,6-triarylpyrylium salt to the corresponding arene by the catalyst-free condensation reaction with sodium phenylacetate (Fig. 1), the backbones of macrocycles with functional groups at various positions can be achieved in a few steps with moderate yields. Also, since the entire structures were based on neutral backbones, these non-charged arenes can be readily separated and purified by chromatography.

Xiaopeng Li received his BS degree in chemistry from Zhengzhou University in 2004 and PhD degree from Cleveland State University in 2008. After postdoctoral training at University of Akron from 2009 to 2012, he started his independent career as an Assistant Professor at Texas State University. In 2016, he moved to University of South Florida, and was promoted to Associated Professor with tenure in 2019. In 2020, Dr Li returned to China and joined Shenzhen University as the Tencent Founders Alumni Professor. His major research interests include mass spectrometry, supramolecular chemistry based on coordination-driven self-assembly, and supramolecular materials. He was awarded the 2019 Cram Lehn Pedersen prize in supramolecular chemistry from the Royal Society of Chemistry.

In recent years, Li and co-workers have further employed pyrylium salts for the construction of discrete metallo-supramolecules based on the coordination-driven self-assembly of multitopic pyridinium salt building blocks.[27] Through the transformation of pyrylium salts to corresponding pyridinium salts with high yields, the synthetic challenges of multitopic ligands have been overcome with a remarkably simplified process. Also, the feasible separation and characterization were developed for the building blocks with multiple positive charges. Moreover, the modular synthetic strategy[28] and *in situ* one-pot approach[29] were further explored to simplify the synthesis of multitopic ligands using pyrylium salt chemistry.

In this perspective, we attempt to summarize the representative efforts on synthesizing and self-assembling complex macrocyclic and metallo-supramolecular architectures using pyrylium salt chemistry. Two different types of systems are included in this perspective, *i.e.*, organic macrocycles and metallo-supramolecules. Among these architectures, 2,4,6-triphenylpyrylium salts (TPP) and its derivatives have been widely used as the key precursor due to their facile transformation to 1,2,3,5-tetraarylbenzene derivatives or 1,2,4,6-tetraphenylpyridinium derivatives (Fig. 1). With rigid structures and well-defined angles, such intermediates could serve as ideal backbones of macrocycles and metallo-supramolecules, as well as the scaffolds for facile functionalization at various positions. We wish that this perspective not only highlights the recent achievements in pyrylium salt chemistry, but also inspires the community to revisit this chemistry to design and construct macrocycles and metallo-supramolecules with increasing complexity and desired function.

2. Pyrylium salts and their synthetic methods

Since the discovery of pyrylium salts, numerous synthetic methods have been developed for the synthesis of pyrylium salts. Herein, we emphasize three major synthetic approaches (Fig. 2) to achieve the 2,4,6-triarylpyrylium salt (TPP), which has

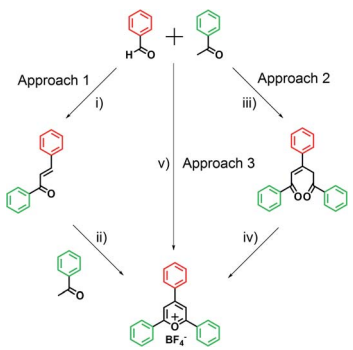

Fig. 2 Three common synthetic approaches to 2,4,6-triarylpyrylium salt; (i) NaOH, EtOH, rt; (ii) HBF_4, 1,2-dichloroethane, reflux; (iii) NaOH, EtOH, reflux; (iv) Ph_3COH, HBF_4, Ac_2O, rt; (v) $BF_3{\cdot}Et_2O$, 100 °C.

been widely used as the precursor in constructing macrocyclic architectures.

In approach 1, the precursor of *trans*-chalcone was first prepared by a condensation reaction between benzaldehyde and 1 equivalent of acetophenone in the presence of a strong base, *e.g.*, sodium hydroxide. Then, another equivalent of acetophenone reacted with the intermediate through dehydrocyclization to obtain the target salt.[30] Although multiple steps were involved, this approach enabled the synthesis of dissymmetrical pyrylium salts by using different ketones in two steps. 2,4,6-Triphenylpyrylium salts can also be prepared with the 1,5-diketone method (approach 2), in which 1,5-diketone was synthesized as the precursor by treating benzaldehyde with 2 equivalents of acetophenone under a basic condition. Then, the ring-close reaction was achieved by addition of triphenylmethanol and strong acids to obtain the pyrylium salt with relatively higher yield than the other two approaches.[31] The third synthetic approach offers a more efficient preparation by treating benzaldehyde and 2 equivalents of acetophenone with $BF_3 \cdot OEt_2$ in a one-pot condensation reaction.[32,33] However, this approach is performed with a strong acid at high temperature, which may result in undesired products for some reagents. It is worth noting that due to the ionic feature of pyrylium salts, these compounds are insoluble in many organic solvents like toluene or diethyl ether, and can be easily purified by washing with such solvents.

3. Heterocyclic molecules based on pyrylium salts

With the positively charged oxygen atom, pyrylium salts are strongly reactive towards diverse nucleophiles to readily form various heterocyclic groups, including furan,[7] pyridines,[34] phosphinines,[35–37] pyridinium salts,[38,39] thiopyrylium salts[40] and betaine dyes[41,42] (Fig. 3). As a result, pyrylium salt chemistry provides a versatile platform for constructing different types of small molecular aliphatic,[43,44] aromatic,[45] and heterocyclic[46–48] derivatives with broad applications.[49–53]

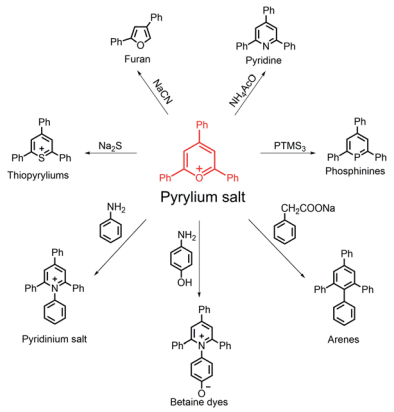

Fig. 3 Synthesis of heterocyclic compounds using pyrylium salts as precursors. The counterions are omitted.

4. Polymers based on pyrylium salts

In addition to the synthesis of various small molecular heterocyclic derivatives, pyrylium salts are involved in the preparation of polymers with pyridinium moieties. Besides the usage as photocatalyst and initiator in many polymerization processes,[54,55] pyrylium salts themselves are widely used as the building blocks of many one-dimensional (1D) and two-dimensional (2D) polymers (Fig. 4). By utilizing the bis-pyrylium salts and diamines, the condensation reaction between them can lead to a polymerization process, and introduce the charged pyridinium ring into the backbone (**1** in Fig. 4a). Alternatively, the ionic polymers can also be obtained by introducing a betain dye moiety into the side chain, and be polymerized by other functional groups (**2** in Fig. 4a).

Another type of polymer was prepared using pyrylium salts as the synthetic intermediates to form different neutral conjugated structures (**3** and **4** in Fig. 4b). Different functional polyamides, polyesters and polyethers were prepared with violet and/or blue photoluminescence in both solution and solid

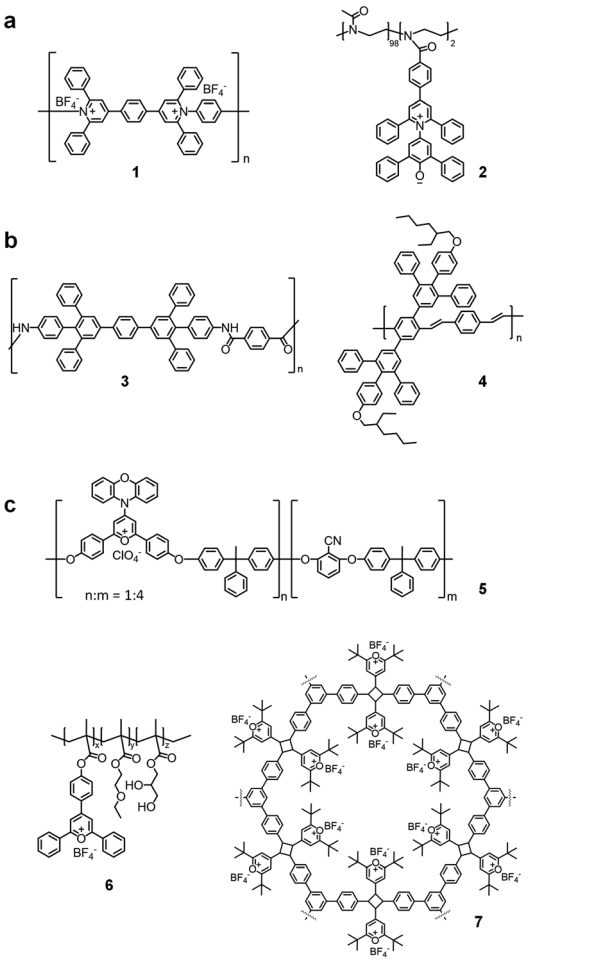

Fig. 4 Different types of polymers prepared by pyrylium salt chemistry. (a) Polymers with pyridinium salts in structures. (b) Polymers with neutral conjugated structures. (c) Polymers with pyrylium rings remaining in the structures.

state.[56–61] The facile synthesis process of the pyrylium salts simplifies the introduction of functional groups onto the backbones and side chains, and also facilitates the tuning of the polymers' solubility, stiffness and function.

The third type of polymer was prepared using the pyrylium ring itself as the structural moiety without transformation to other heterocycles (**5** (ref. 62) and **6** (ref. 63) in Fig. 4c). Benefiting from the remaining positively charged oxygen atom, the pyrylium rings are highly electrophilic and reactive to many nucleophilic chemicals with a wide range of absorptions and emissions.[63–66] Interestingly, styryl pyrylium salts were found to have topochemical dimerization under photoirradiation to form head-to-tail cyclobutyl rings in crystalline form ref. 67. Due to this specific feature, the single-crystal structure of the 2D polymer was obtained by photochemically induced polymerization of the tris-pyrylium salt monomer without losing the ordered structure within the crystal (7 in Fig. 4c).[68] In addition, this pyrylium-containing polymer could be converted into another 2D polymer with pyridines by simple exposure to gaseous ammonia.[69]

5. Organic macrocycles based on pyrylium salts

In the past half century, macrocycles have attracted considerable attention not only in the modification of natural macrocycles like cyclodextrins,[70,71] porphyrins,[72–74] and their derivatives, but also in the synthesis of artificial macrocycles such as crown ether,[75,76] calixarenes,[77] cucurbiturils,[78] pillararenes,[79,80] cyclic benzenoids,[81,82] and other macrocycles.[83] Functionalized macrocycles have been widely used in molecular machines,[84,85] biomedicine,[86,87] catalysis,[71,88,89] binding and purification,[81] anion recognition,[90] molecular sensing,[91–93] and other applications. Among them, shape-persistent macrocycles have become ideal systems to study the structure–function relationships at the nanoscale level on account of their rigid structures, inherent stabilities and precisely-controlled sizes and shapes.[94–97] However, the preparations of many macrocycles are time-consuming, and suffer from the tedious separation and purification, as well as low yields.

For the conventional approaches to shape-persistent macrocycles, many synthetic methods have been explored, including the intermolecular coupling reaction between monomers,[98–104] and the intramolecular cyclization of long linear precursors.[105–107] The former strategy involved just a one-step reaction. However, byproducts with different membered rings are inevitable, leading to a tedious separation process and quite low yields (4–6%). The latter strategy gave a higher yield (*ca.* 75%) for the final cyclization step. However, the synthesis of the linear precursor involved multiple steps.[108] Also, it still remains challenging to internally and externally modify the macrocycles with functional groups for potential applications.

In 2002, Höger and co-workers first reported the preparation of a shape-persistent macrocycle based on pyrylium salt

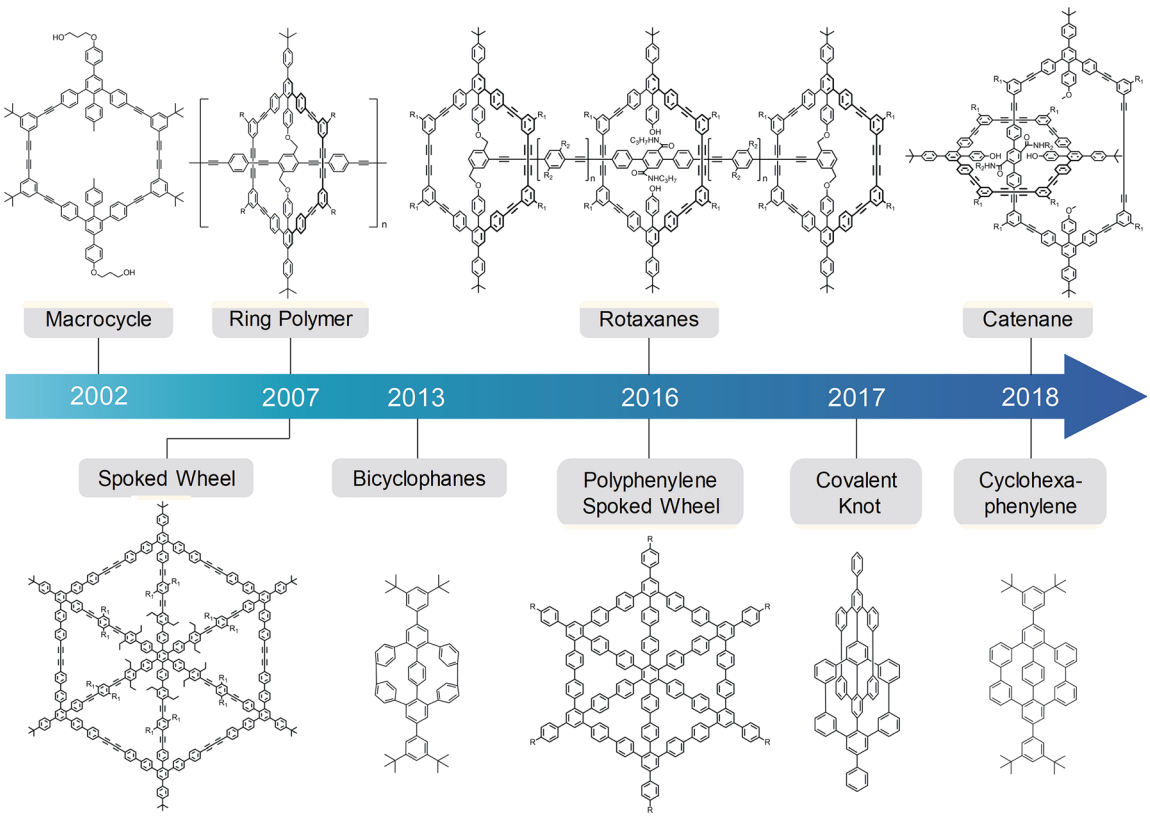

Fig. 5 Development of discrete organic macrocycles prepared by pyrylium salts.

chemistry.[109] Such salts could be easily obtained through facile processes with large quantities and diverse functional groups at different positions.[110] Also, the catalyst-free transformation from pyrylium salts to the corresponding arenes was able to form rigid structures with up to four directions, and thus became a powerful synthetic approach for constructing discrete macrocycles (Fig. 5). Such a key transformation had a high tolerance to halogen groups, thus simplifying the synthesis without tedious protecting and deprotecting reactions. Finally, this strategy enables facile functionalization inside and outside the macrocycles with desirable properties and functions.[111]

5.1 Shape-persistent macrocycles

As shown in Fig. 6, this strategy utilized 2,4,6-triarylpyrylium salt as the key precursor to build the directing unit for further constructing the macrocycles. Among the four phenyl rings substituted on the directing arms of **10**, Ph^A and Ph^C usually act as the anchoring sites for the internal and external modification of the target macrocycles, respectively. The other two phenyl groups of Ph^B were substituted with halogen atoms for further elongation process by Sonogashira coupling of two corner spacers **11** with mono-protected bisacetylene. After the deprotecting process, the cyclization was performed with Glaser reaction between two half-rings **13**, and the macrocycle **14** could be obtained with yields of around 50%. Moreover, with the decoration of flexible alkyl chains on the outside, the macrocycles could self-assemble into highly ordered monolayers on the surface of highly oriented pyrolytic graphite (HOPG). As shown in Fig. 6b, three different domains of **14** separated by domain boundaries were observed using scanning tunneling microscopy (STM). High-resolution STM imaging revealed that the macrocycles were tilted from the direction of the molecular rows (Fig. 6c), and a tentative packing model of such pattern is shown in Fig. 6d.

By using this strategy, a series of shape-persistent macrocycles was synthesized with different shapes and sizes. Furthermore, with additional modifications inside or outside the macrocyclic backbones, self-assembled monolayers of the macrocycles on the surface were well-controlled with a wide range of symmetries and periodicities.[112–116] However, in this synthesis process, the byproducts of the cyclic trimers, oligomers, and polymers were still inevitable, which hampered the efficiency of the reaction and further separation process.

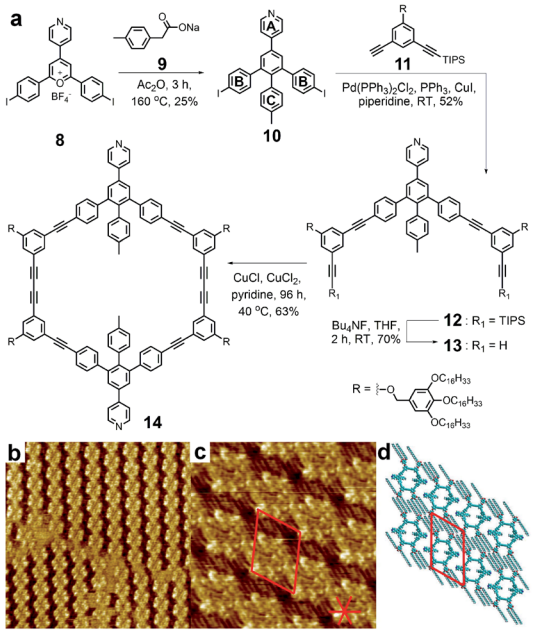

Fig. 6 Macrocycle based on pyrylium salt chemistry. (a) Synthesis of macrocycle **14**. (b) STM image of **14** self-assembled at the 1,2,4-trichlorobenzene/graphite interface. (c) High-resolution STM image with unit cell and the orientations of the graphite surface indicated in red. (d) Schematic representation of the tentative packing model with the corresponding unit cell. Adapted with permission from ref. 115.

5.2 Macrocycles by template-directed cyclization

In order to increase the yield of macrocycles and eliminate the formation of byproducts, a new strategy based on template-directed cyclization was developed (Fig. 7). Through this strategy, the cyclization reaction can be optimized to avoid other oligomers or polymer byproducts, leading to a high yield of up to 90%.[117] In the synthesis, two half-rings were bridged together with a soft linker through the Ph^C moiety on the tetraphenyl benzene backbone. With the two half-rings linked, the final cyclization could be controlled as an intramolecular reaction and dramatically reduce the formation of other byproducts. Moreover, the central linker units were able to provide additional reaction sites for further synthesis of more complex architectures.

5.2.1 Ring polymers. Many examples have shown that the macrocycles can assemble into 2D arrays or stack into tubular

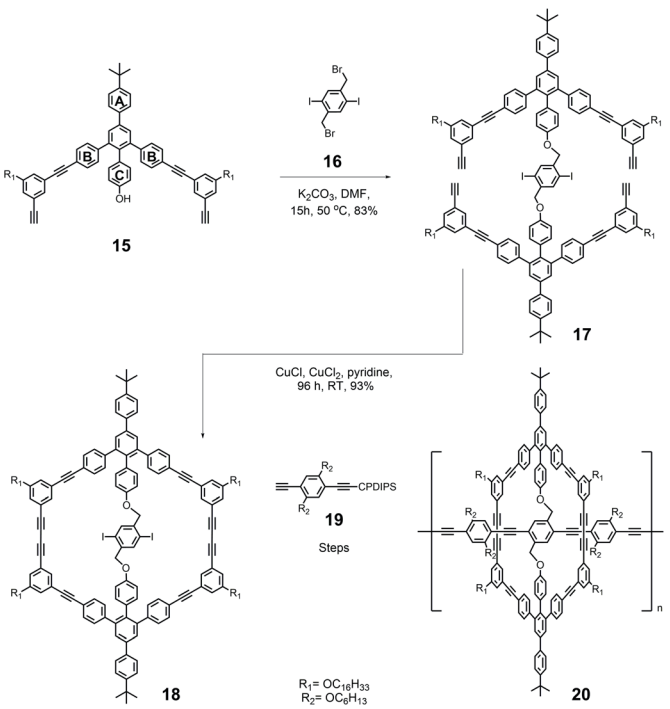

Fig. 7 Synthesis of ring polymer **20** based on pyrylium salt chemistry through flexible template-directed synthesis.

structures.[118,119] However, the supramolecular aggregates are generally fragile to solvent and temperature. A new type of ring polymer was reported by Höger and Lupton, in which the macrocycles were threaded perpendicularly with covalent connections inside (Fig. 7).[120] By using the strategy of the template-directed cyclization and connecting the template linkers between the macrocycles, this new type of polymer was synthesized by linking a linear conjugated axle inside with a string of orthogonally aligned macrocycles. In the detailed synthesis process, phenol groups were introduced on the Ph^C benzene of the half-ring **15**, and two half-rings were connected together with the central linker **16** by stable ether bonds. With the iodide on the central linker of **18**, straight mono-protected bisacetylene **19** was installed by Sonogashira coupling to form the central axle after the cyclization of the two half-rings. Then, these new terminal alkynes were deprotected and polymerized by Glaser coupling to achieve the final ring polymer **20**.

By comparing the photoluminescent properties of the ring polymer and the ring itself, it was found that the macrocycle-encapsulated polymer could accumulate the excitation energy of the rings and worked efficiently as a light-harvesting material. Also, with the macrocycles cladding outside, the ring polymer exhibited much higher rigidity compared with the bare linear polymer alone. Conventional linear polymers often become flexible and folded with long chains, and a large deviation was observed when testing the polarization anisotropy. In sharp contrast, the ring polymers could maintain the rigidity even with high molecular weight, leading to a potential application as a molecular ruler for the calibration of GPC.[121]

5.2.2 Rotaxane. Based on the design of the ring polymer, a nanosized phenylacetylene rotaxane was synthesized through a template-directed approach by Grimme and Höger.[122] In the structures **21a** and **21b** (Fig. 8), two shape-persistent macrocycles were incorporated as the stopper of the rotaxane *via* stable ether linkers. Conversely, the central rings were linked to the template with ester bonds, which could be dissociated by nucleophilic substitution. As such, the final rotaxane with both shape-persistent ring and rigid axis were obtained.

Both the stoppers and the central ring are shape-persistent macrocycles with the exact same shape and size. The *tert*-butyl and alkoxy groups were also installed on the exterior of each ring to avoid the unthreading of the central macrocycle. However, it was found that the central ring could unthread through the axis and stopper spontaneously, leading to the disassembly of the rotaxane. Further theoretical DFT calculations revealed the detailed unthreading process. With the flexible linker dragging by the axle, the stopper ring could fold like a taco and the expanding central macrocycle could slip off from the rotaxane axle. This unthreading process revealed that the shape-persistent macrocycles with flexible templates were not as rigid as expected. Instead, rigid templates might enhance the shape persistence of stoppers for maintaining the rotaxane structures.

5.2.3 Catenane. Inspired by the successful synthesis of rotaxanes, such a covalent template approach was also used for the construction of interlocked catenane **22**.[123] In this design (Fig. 8), the central covalent linker not only facilitated the cyclization of the first ring, but also became the edge of the second ring. After a similar ester cleavage, the final mechanically interlocked catenane was obtained. The key synthetic step was the construction of the second ring, for which the phenyl groups were extended from the template center to reduce the steric hindrance for the subsequent coupling reaction, then two mono-protected half-rings were connected to the template of the first ring with the pre-substituted aryl iodides. Eventually, similar deprotection and cyclization steps were carried out to achieve the final catenane. The syntheses of rotaxanes and catenane have proved that pyrylium salt chemistry coupled with template-directed strategy could significantly advance the design and synthesis of sophisticated architectures with mechanical bonds.

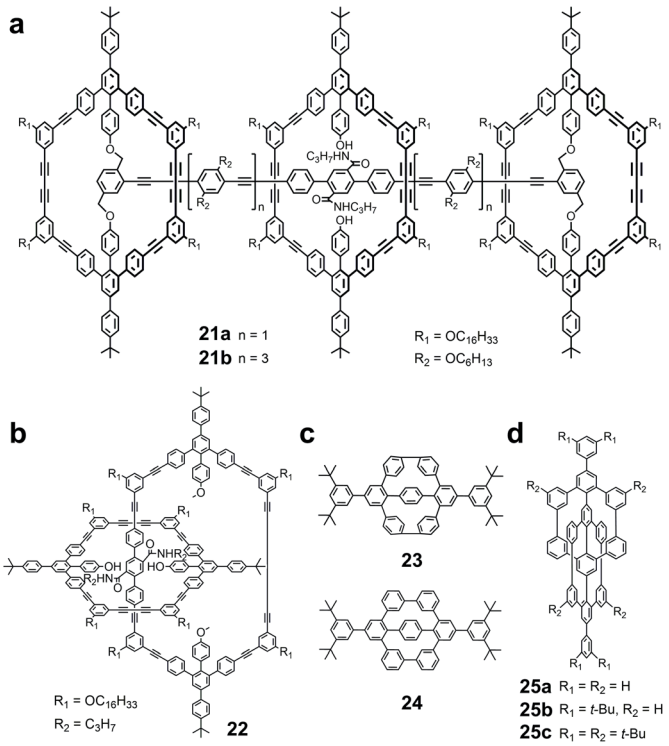

Fig. 8 Chemical structures based on pyrylium salt chemistry and template-directed strategy. (a) Rotaxanes; (b) catenane; (c) phenylene bicyclophanes; (d) covalent knots.

5.2.4 Phenylene bicyclophanes. Numerous cases have proved that flexible linkers can be used as a template for constructing macrocycles efficiently. However, in most of them, the resulting macrocycles were unable to provide sufficient rigidity for further study, such as self-assembly. Therefore, rigid units have emerged as alternative templates for the construction of macrocycles. Different from the synthetic strategy using flexible linkers, the rigid template was installed with multiple sodium acetate groups, and the linking process of the backbones was directly achieved by the multifold condensation reactions between the templates and pyrylium salts. Given the short length of the templates, the distance between the two backbones could be very close. Therefore, the final cyclization could

be simply carried out by Yamamoto coupling reaction between the adjacent halogen atoms on the two backbones.

By using this strategy, several high strained phenylene bicyclophanes with different central templates were reported by Grimme and Höger (**23** in Fig. 8).[124] Pyrylium salts with bromide atoms substituted on the *para*-position of Ph^B were used as the precursors. Since the adjacent bromide atoms were oriented into different directions, a large strain energy was built up during the cyclization process. Due to the compacted structures and high strains in the macrocycles, the central aromatic units and four benzene rings of the bicyclic backbone were forced to be perpendicular to the molecular plane. Interestingly, although the high strain energy was built up during the cyclization process, the final Yamamoto reaction was still able to reach an astonishing yield up to 80%. After deposition on HOPG, these aromatic units were oriented vertically to the graphite surface, and thus offered a potential solution for volume-phase surface functionalization.

Using the same synthetic strategy based on pyrylium salt chemistry, Müllen *et al.* reported a cyclohexa-*meta*-phenylene (**24** in Fig. 8) as a precursor for the synthesis of hexa-*peri*-hexabenzocoronene (HBC).[26] Different from Höger's design, chloride atoms were incorporated into the *meta*-position of the pyrylium backbones. Thus, after the two-fold condensation reaction, chloride atoms were aligned face to face to enable the subsequent cyclization by Yamamoto coupling. Although the final cyclohexa-*meta*-phenylene had much less strain energy in the structure, the central phenylene group and four phenylene units still created a torsion angle to the molecular plane due to the steric hindrance brought by hydrogen atoms on the benzene rings. By flattening the phenylene units, the transformation to HBC was achieved within just a few seconds, producing a high yield of 89%. This work offered a new approach for the synthesis of 2D nanographene by the flattening of three-dimensional (3D) oligo- and polyphenylenes.

In addition to phenylene bicyclophanes, the same strategy with rigid templates was used to construct 3D carbon nanostructures with increasing complexity, for instance, covalently interlocked cyclohexa-*meta*-phenylenes (**25a–c** in Fig. 8).[125] Instead of the mechanical bond of catenanes, this paddlewheel-shaped molecule consists of two cyclohexa-*meta*-phenylene rings, which are orthogonal to each other, but covalently interlocked. Within each cyclohexa-*meta*-phenylene, the central rigid template also serves as a part of rigid hexaphenyl backbone. To achieve this complex structure, the key template dicarboxylate was designed with four chloride atoms orthogonally aligned and pointing outward for further coupling reactions. After a similar condensation reaction with pyrylium salts, the octachloro-precursor was converted into the final paddlewheel structure through a 4-fold Yamamoto coupling reaction of preorganized face-to-face *meta*-chloro-phenylene units. Interestingly, **25a** is extremely thermally stable up to 450 °C, and these 3D nanostructures can subsequently assemble into a tight, stable hierarchical structure with supramolecular interaction. This work further supported the versatility of the pyrylium salt chemistry in the synthesis of complex molecular architectures, and paved a new avenue towards 3D carbon materials by combining the molecular and supramolecular approaches.

5.3 Spoked wheels

By using a template-directed strategy, the cyclization efficiency was substantially improved. However, with the increasing sizes of the macrocycles, these cyclic constructs lost their shape-persistence. Thus, another type of reinforced 2D architecture was reported in 2007 (ref. 126) with a central hub unit and six spokes to enhance the rigidity, and was named as a molecular spoked wheel (**34** in Fig. 9). These disc-shaped molecules exhibited the desired shape-persistence and reasonable solubility.

The synthesis of spoked wheel **34** was also achieved by template-directed approach. The target spoked wheel structure was constructed from different rigid subunits (Fig. 9), *i.e.*, hexaiodo-substituted center **31** as the hub, long and straight phenylacetylene **29** as the spoke, and functionalized arene converted from pyrylium salt **26** as the backbone. In the structure of backbone **26**, two Ph^B groups acted as the key components for further elongation and coupling to form the rim **28**. Ph^C was utilized as the docking site to the central hub unit **31** through the rigid linear spokes **29** to obtain the star-shape precursor **32**, which contains the template within the structure. The final rim closure was achieved by 6-fold intramolecular coupling of adjacent alkyne units on the rims to give the spoked wheel **34** with 65% yield. The structure of the spoked wheel was confirmed by STM on the surface of HOPG using a solution of **34** in toluene (Fig. 9b). The shape and size of the spoked wheel both matched well with the modeling structure (Fig. 9c). Furthermore, the well ordered self-assembly patterns of spoked wheel **34** were observed both at the air–solid (toluene solution deposition) and liquid–solid (octanoic acid/graphite) interface. Due to the different staggering patterns of the *tert*-butyl groups on adjacent molecules, spoked wheel **34** could form two kinds of closed-packing domains with different orientational chiralities on the surface (Fig. 9d–f).

By utilizing this strategy, several spoked wheels were constructed with different sizes from 5.7 to 12 nm. Also, functional groups were introduced at different positions, such as the rim, hub and spoke. As such, the self-assembly of such spoked wheels on the surface could be further controlled with different patterns and symmetries.[127–131] Compared to the structure of the hollow-centered macrocycles, the rigidity of the spoked wheel was highly improved. However, it was found that the spoked wheels based on poly(*p*-phenylene ethynylene)s decomposed slowly at room temperature.[132]

In order to increase the stability of the spoked wheels, another synthetic strategy was established by Müllen and Höger independently in recent years.[25,132] The new types of spoked wheels were build up based on poly(*p*-phenylene)s instead of poly(*p*-phenylene ethynylene)s with the purpose for enhancing the stability and rigidity. In contrast to the previous synthesis (Fig. 10), spoke **36** was attached onto **35** directly through Suzuki coupling on Ph^C with one acetylene in the center. The key star-

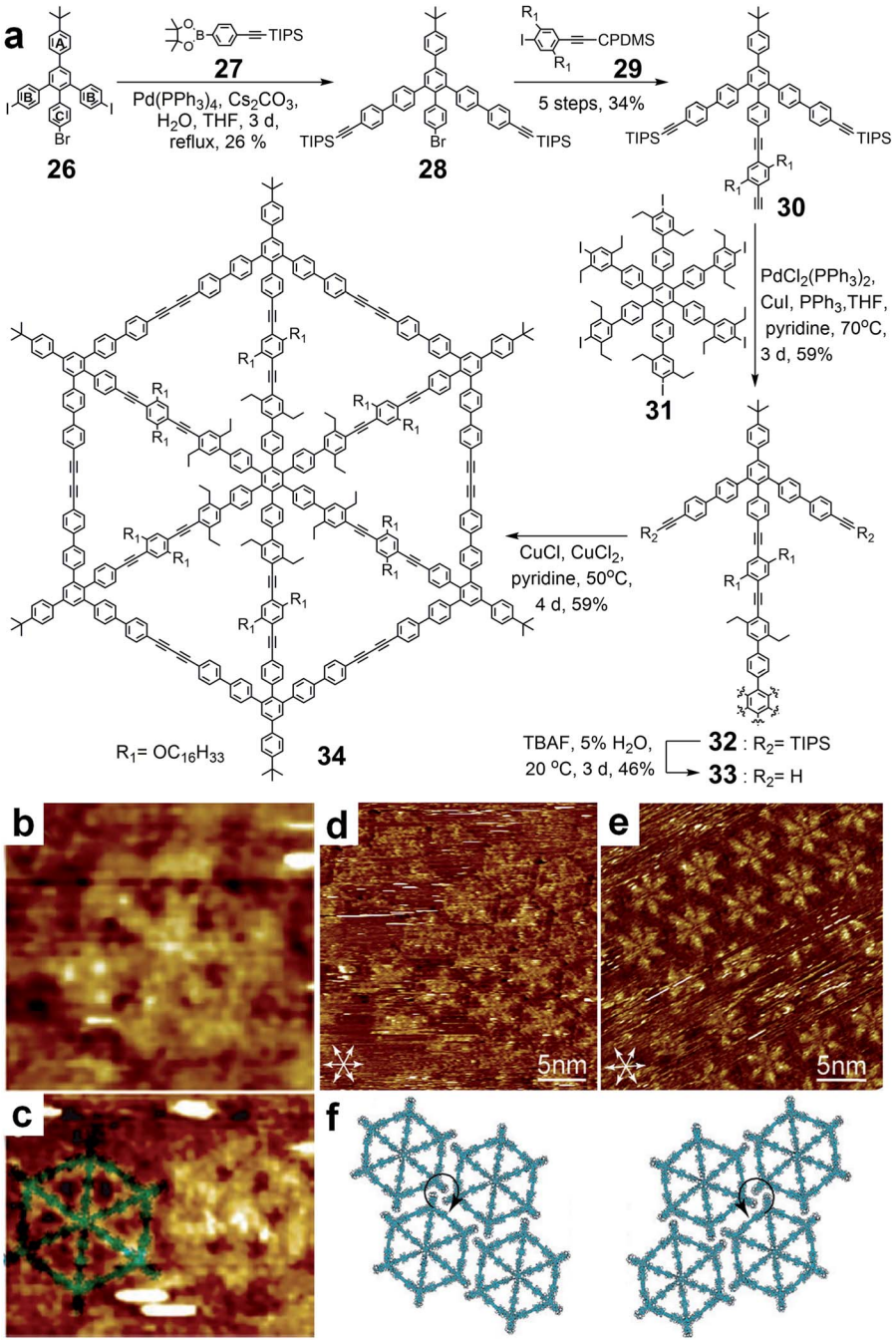

Fig. 9 Synthesis of phenylene ethynylene-based spoked wheel **34** using pyrylium salt chemistry. (a) Synthetic route of spoked wheel **34**; (b) STM image of single spoked wheel **34** on graphite; (c) STM image with molecular model overlapped on the left molecule; (d) STM images of the 2D organization of **34** at the octanoic acid/graphite interface with clockwise staggering; (e) 2D organization of **34** with counter-clockwise staggering; (f) corresponding molecular models of (d) and (e). Adapted with permission from ref. 126 and 128.

shaped precursor **38** was obtained from the Co-catalyzed trimerization of the dimer segments **37** with a relatively high yield of up to 46%. Also, no more elongation was needed for the two arms on Ph^B to facilitate intramolecular Yamamoto coupling in the formation of spoked wheel **39**. The structure of this wheel-like macrocycle was confirmed by forming a self-assembled monolayer and imaging with STM. In addition, the submolecular features of the aromatic frames were clearly observed in the high-resolution STM image (Fig. 10b). A molecular model (Fig. 10c) that was built based on the experimental patterns indicated that the adjacent molecules possibly had interactions through the van der Waals forces of the dodecyl chains installed on the corners. Within the enlarged STM images, the shape and size of the spoked wheel matched closely with the theoretically calculated structure (Fig. 10d and e).

By introducing different side chains on the corner or on the edge of the spoked wheel, Höger also synthesized three all-phenylene spoked wheels using the same strategy. Self-assembled monolayers at the 1-phenyloctane (PHO)/HOPG interface with different 2D crystalline patterns were also investigated by STM with submolecular resolution. One of the three spoked wheels (**40** in Fig. 10f) installed with six tris(hexadecyloxy)benzyl groups could form an unusual interdigitation pattern, which is formed by three crystallographically different molecules with a rather large unit cell (Fig. 10g). These new spoked wheels exhibited high stability and rigidity even in a wide temperature range, as well as a liquid crystalline feature.[132] The synthetic strategy could offer a promising pathway for the design and synthesis of new 2D carbon materials and liquid crystalline materials.

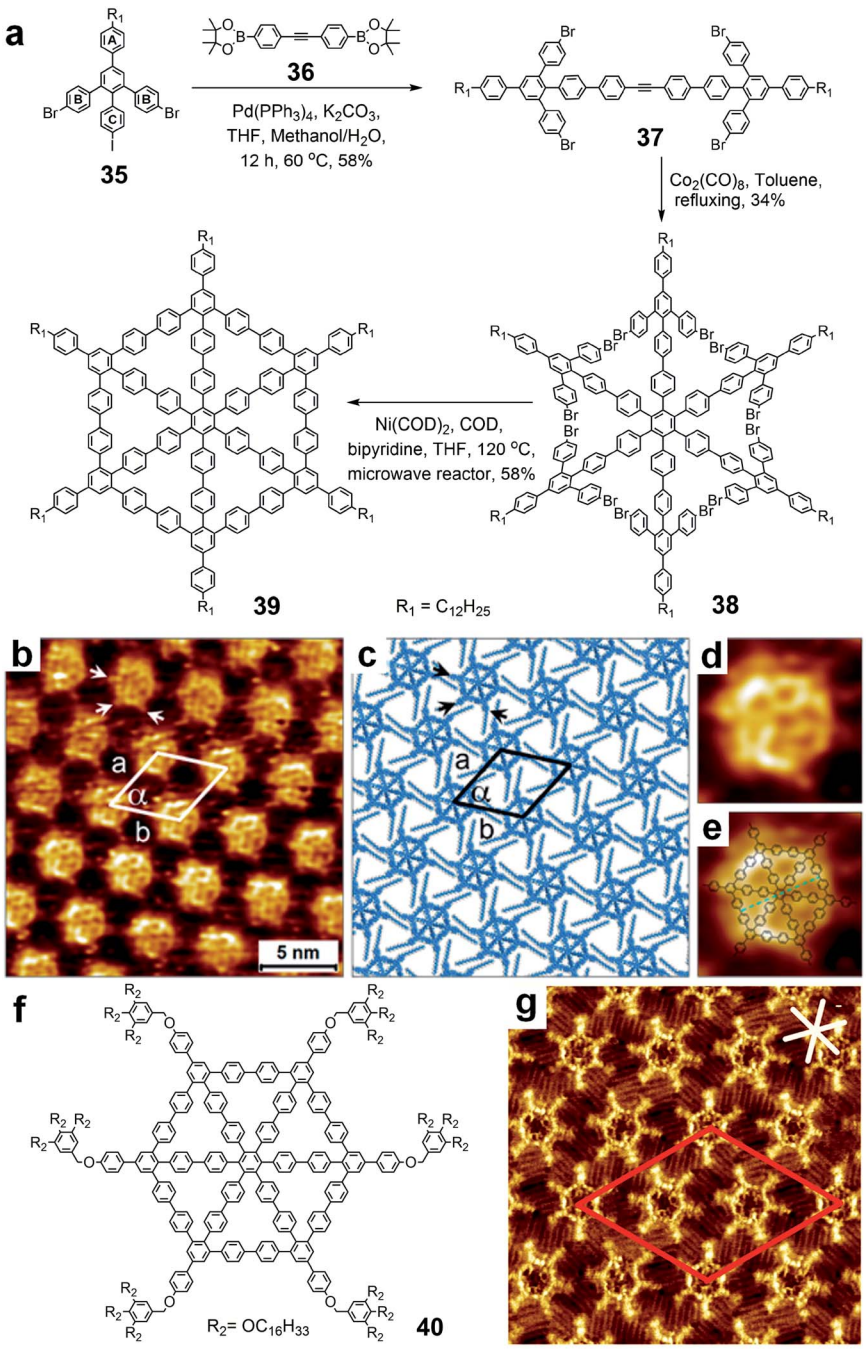

Fig. 10 Synthesis of phenylene-based spoked wheels using pyrylium salt chemistry. (a) Synthetic route of spoked wheel **39**; (b) high-resolution STM image of a self-assembled monolayer of **39**; (c) molecular model of the self-assembled network of **39**; (d) enlarged STM image of a single molecule of **39**; (e) enlarged STM image overlapped with the molecular structure of **39**; (f) structure of spoked wheel **40**; (g) STM image of self-assembled monolayer of **40**. Adapted with permission from ref. 25 and 132.

6. Metallo-supramolecules based on pyrylium salt chemistry

By utilizing the coordination-driven self-assembly with metal ions (acting as corner or node), the construction of complex architectures can be dramatically simplified. Due to the highly directional and predictable feature of metal coordination, the sizes and geometries of the 2D and 3D metallo-supramolecules can be pre-designed and precisely controlled. Since the 1990s,[133] numerous metallo-supramolecules have been constructed with elaborate architectures and desired functions.[134–153] However, because of the bending arms of the ditopic ligands and the distortion of the coordination sites in large scale systems, unexpected constructs and byproducts with different number rings have become the obstacles in the self-assembly of metallo-supramolecules.[154–159] Unfortunately, unlike the organic macrocycles, it is challenging to separate the metallo-supramolecules using chromatography due to the highly charged structures and the dynamic coordination bonds. Thus, new synthetic strategies are highly desirable for the preparation of metallo-supramolecules with increasing complexity.

To precisely control the self-assembly to be the single component process through rational design, Li and co-workers established the multivalent coordination-driven self-assembly guided by increasing the density of coordination sites (DOCS) to introduce more geometric constraints for the formation of discrete metallo-supramolecules.[160] In order to increase the DOCS, extra parallel arms could be installed on the backbones of the ligands to reinforce the rigidity of the structure. These multitopic ligands could further ensure the angle between the arms, and work cooperatively to eliminate the formation of undesired byproducts. Thus, multivalent coordination-driven self-assembly emerged as a powerful approach for the construction of giant metallo-supramolecules with increasing complexity and stability (Fig. 11). Similar to the organic macrocycles, in the synthesis of multiarmed ligands, phenylene or phenylene–ethynylene were widely incorporated into the backbones of the building blocks in many cases, and coupling reactions were utilized to extend arms to different orientations with corresponding binding subunits.[160–164] However, with the increasing complexities and sizes of the structures, it remains a formidable challenge to prepare multitopic ligands due to the relatively low reaction efficiency on multiple sites, tedious synthesis process and difficult purification process of high polarity products. In the journey of pushing the limits of complexity, pyrylium salt chemistry was employed to prepare a series of multitopic terpyridine (tpy) building blocks with high efficiency.

6.1 Concentric hexagons assembled by multitopic ligands

To overcome the synthetic challenges, a series of tetratopic tpy ligands was prepared by condensation, followed by Suzuki coupling strategy (Fig. 12). Briefly, the condensation reaction between pyrylium salts and primary amines was first employed to simplify the preparation of multitopic ligands.[27] Compared to the condensation between pyrylium salts and sodium

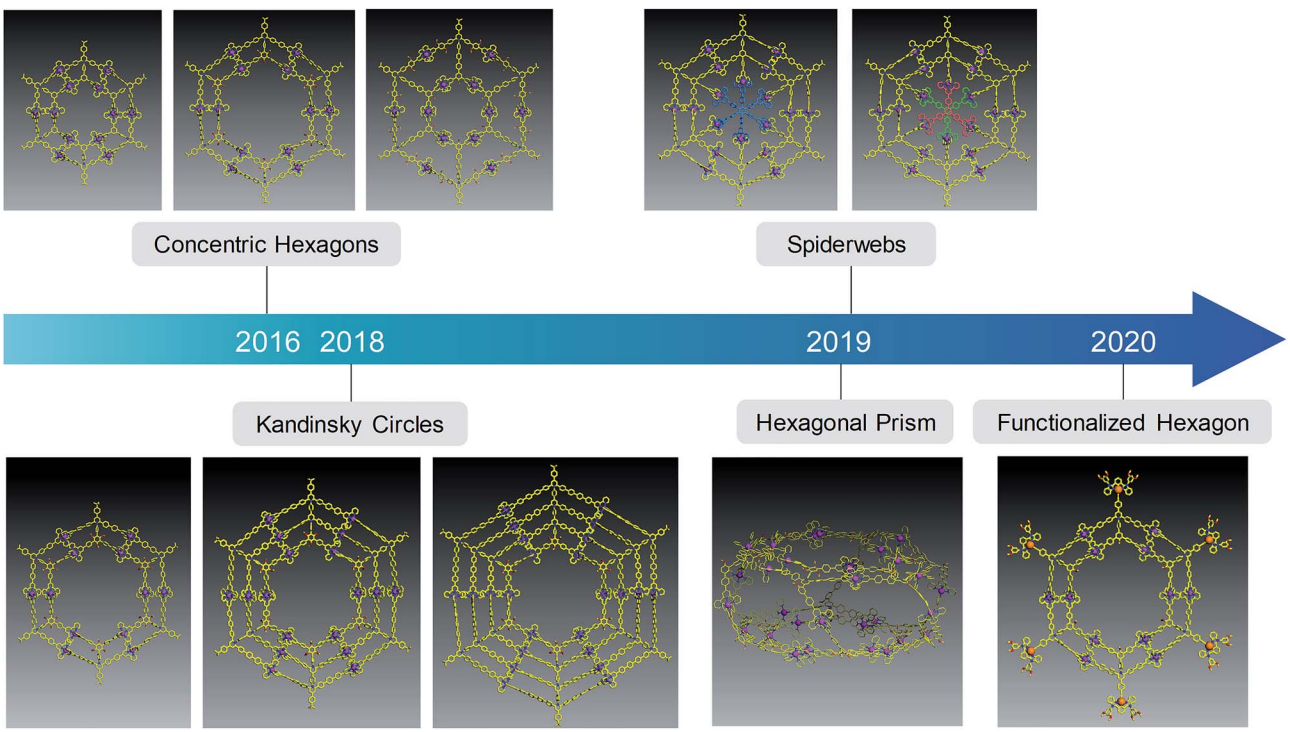

Fig. 11 Development of metallo-supramolecules assembled by multitopic terpyridine ligands prepared by pyrylium salt chemistry.

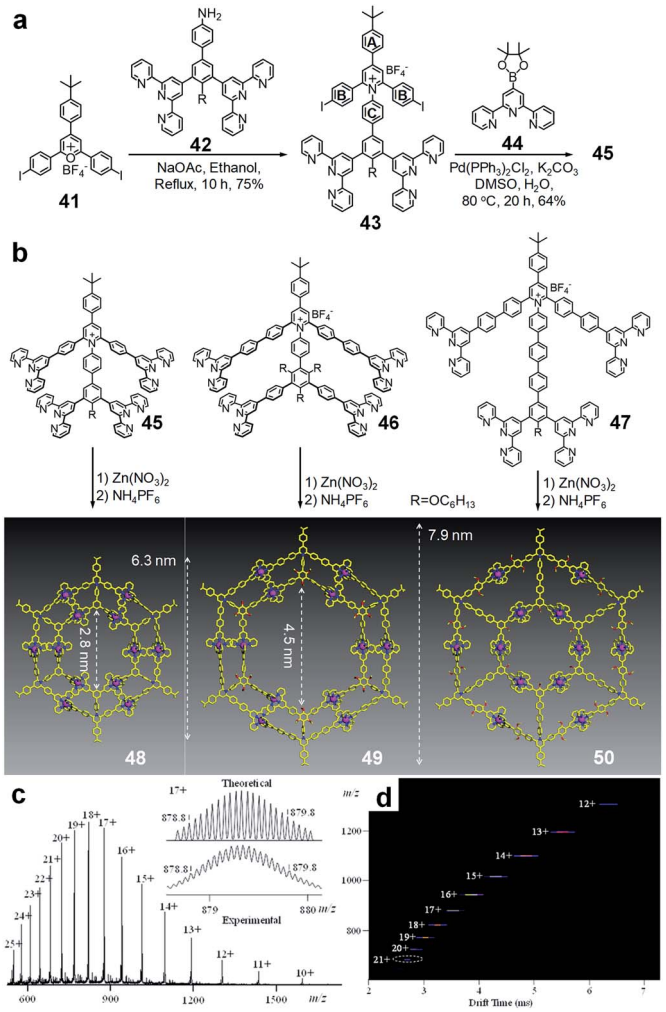

Fig. 12 Self-assembly of concentric hexagons by tetratopic tpy-pyridinium salt ligands prepared by pyrylium salt chemistry. (a) Syntheses of tetratopic ligands by condensation, followed by Suzuki coupling reaction; (b) self-assemblies to concentric hexagons; (c) electrospray ionization-mass spectrometry (ESI-MS) and (d) ion mobility-mass spectrometry (IM-MS) characterization of **49**. Adapted with permission from ref. 27.

phenylacetate, this condensation was able to convert pyrylium salt **41** into pyridinium salt **43** in high yield. After that, a two-fold Suzuki coupling reaction was performed to prepare tetratopic tpy ligand **45** with a yield of 61%.

During the self-assembly, ligand **45** assembled with Zn(II) ions in a 1 : 2 ratio to construct concentric hexagon **48** in nearly quantitative yield. Benefiting from the positive charges of the pyridinium backbones and the metal ions, the molecular mass could be easily confirmed by electrospray ionization mass spectrometry (ESI-MS) with one prominent set of peaks due to the successive loss of counterions (Fig. 12c). Traveling-wave ion mobility-mass spectrometry (TWIM-MS) further indicated that the discrete concentric hexagon was found as the predominant product on account of the highly rigid backbone (Fig. 12d). In contrast, multiple assemblies, including that of the tetramer, pentamer, hexamer and heptamer, were observed for the self-assembly using the ditopic tpy ligand.[165] By using the condensation followed by coupling synthetic strategy to prepare multitopic building blocks, the other concentric hexagons **49** and **50** were assembled using different tetratopic tpy ligands **46** and **47**, respectively (Fig. 12). Also, the combination of different tetratopic ligands could assemble into hybrid concentric hexagons with increasing diversity and complexity.[27] Besides the decent yield during the synthesis, concentric hexagons were able to hierarchically self-assemble into nanoribbon structures on the surface of HOPG, leading to a potential application as nanomaterials for further studies.

6.2 Kandinsky circles constructed by modular synthetic strategy

In the pursuit of constructing higher generations of concentric hexagons, hexatopic and octatopic tpy ligands are needed to achieve the 3rd and 4th generation structures, respectively. However, a synthetic strategy involving condensation followed by coupling was unable to prepare the hexatopic or octatopic building blocks due to the defects generated during the coupling reaction, and the challenge for the isolation of multitopic ligands from a mixture of pyridinium salts with similar polarity.

As such, a modular synthetic strategy was further developed by Li *et al.* to prepare the target ligands in high efficiency.[28] Instead of performing the coupling reaction on pyridinium salts, tpy units were introduced to the Ph^B phenyl groups of pyrylium salts by the Suzuki coupling reaction before the condensation (Fig. 13). Under the basic condition of the Suzuki coupling reaction, the pyrylium rings were opened to form neutral diketones, which were quite stable and readily purified by chromatography. Then, the ditopic units can be converted back to pyrylium salts quantitatively by simply treating with a strong acid, *e.g.*, HBF_4. Using the same process, a series of tpy-containing ditopic modules (**51** to **56**) with different arm lengths was prepared efficiently for the different layers of nested hexagons, namely, Kandinsky circles.

During the synthesis, pyrylium salt modules with amide groups were applied for the condensation. After that, the so-formed pyridinium salt intermediates with amide could be deprotected to generate primary amine for the next round of condensation with the corresponding pyrylium salt module. By repeating the condensation–deprotection cycles, the multitopic ligands were constructed from the inner arms to outer arms. By utilizing this elaborate and powerful strategy, ligands **46**, **59** and **60** have been successfully prepared. Theoretically, higher generations of multitopic building blocks are also feasible by repeating these steps more times.

In the self-assembly with Cd(II), three generations (**61–63**) of Kandinsky circles were assembled with molecular weights of 17 964, 27 713 and 38 352 Da, respectively. Beyond individual metallo-supramolecules, these Kandinsky circles could hierarchically assemble into nanoribbons on the HOPG surface due to the strong interaction between the nested structure and

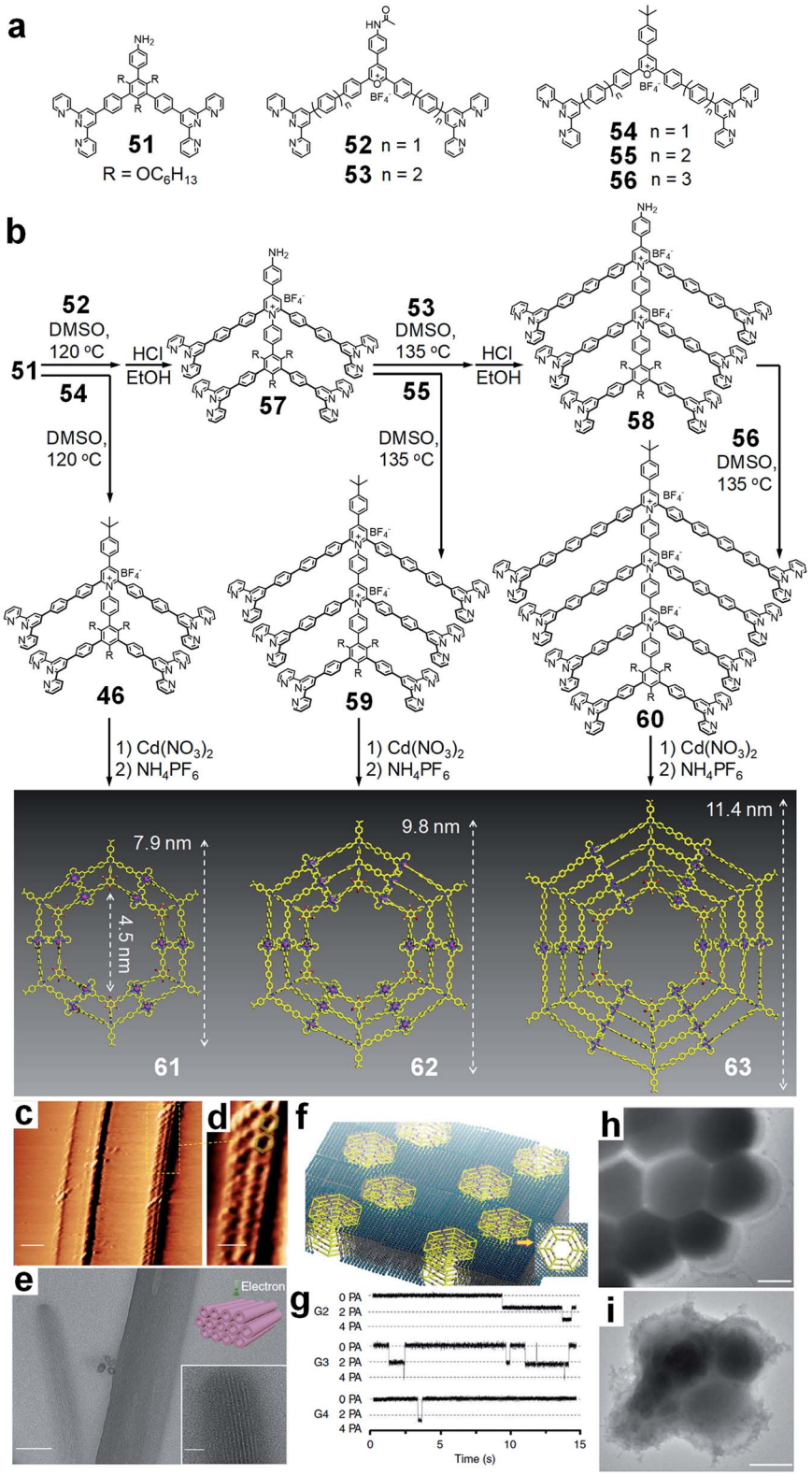

Fig. 13 Metallo-supramolecular Kandinsky circles by modular synthesis. (a) Modules used in synthesis; (b) synthesis and self-assembly to Kandinsky circles; (c) STM images of nanoribbons assembled by **61**; (d) enlarged STM image of nanoribbon structure; (e) TEM imaging of tubular-like nanostructure assembled by **61**; (f) proposed model of transmembrane channels formed by **62**; (g) current traces (15 s) of **61** (5.0 nM), **62** (5.0 nM), and **63** (40 nM) in the planar lipid bilayer at +100 mV in KCl (1.0 M) solution; (h) TEM images of MRSA cells; (i) MRSA cells were treated by **61** and damaged, and cell death was observed. Adapted with permission from ref. 28.

substrate (Fig. 13c and d). Furthermore, these discrete nested metallo-supramolecules were prone to assemble into tubular nanostructures in solution, perhaps on account of the π–π stacking and van der Waals interaction (Fig. 13e). Due to the high density of positive charges and the pyridinium salts containing backbones, these metallo-supramolecules showed strong electrostatic interactions with the negatively charged anionic glycopolymers on the cell wall of Gram-positive bacteria and formed transmembrane channels (Fig. 13f), leading to a high antimicrobial activity against methicillin-resistant *Staphylococcus aureus* (MRSA), but negligible toxicity to eukaryotic cells (Fig. 13h and i).

6.3 Spiderwebs constructed by one-pot synthesis/self-assembly strategy

Although the modular strategy enabled the synthesis of the multitopic tpy ligand, the separation of the charged pyridinium building block was still a major limitation for constructing concentric hexagons. In order to simplify the synthesis process and avoid the separation of multitopic building blocks, a multicomponent synthesis/self-assembly strategy was recently developed by combining the irreversible condensation and highly reversible ligand–metal coordination in one pot[29] (Fig. 14). Given the highly efficient condensation between pyrylium salts and primary amines, the pyrylium salt **54** was mixed with the primary amine precursor **64**, hexatopic tpy ligand **65**, and Zn(II) at a 6 : 6 : 1 : 18 ratio in one pot, in which a pentatopic building block could be generated *in situ* for the self-assembly with **65** and Zn(II) to construct a spiderweb-like 2D metallo-supramolecule **67**. Similarly, two three-armed ligands **66** were applied to replace hexatopic ligand **65** in the combination with **54**, **64** and Zn(II) to construct another spiderweb **68** with two overlapped ligands **66** as the hub. Both spiderwebs were clearly observed by ultrahigh-vacuum, low-temperature scanning tunnelling microscopy (UHV-LT-STM) (Fig. 14b and d). The images showed the hexagon shaped flakes of the individual metallo-supramolecules with the diameters of 7 nm, agreeing well with the modeling structures. Zoomed-in STM images further showed the submolecular structures of both spiderwebs. Accordingly, three signal lobes in the center of **68** and six lobes

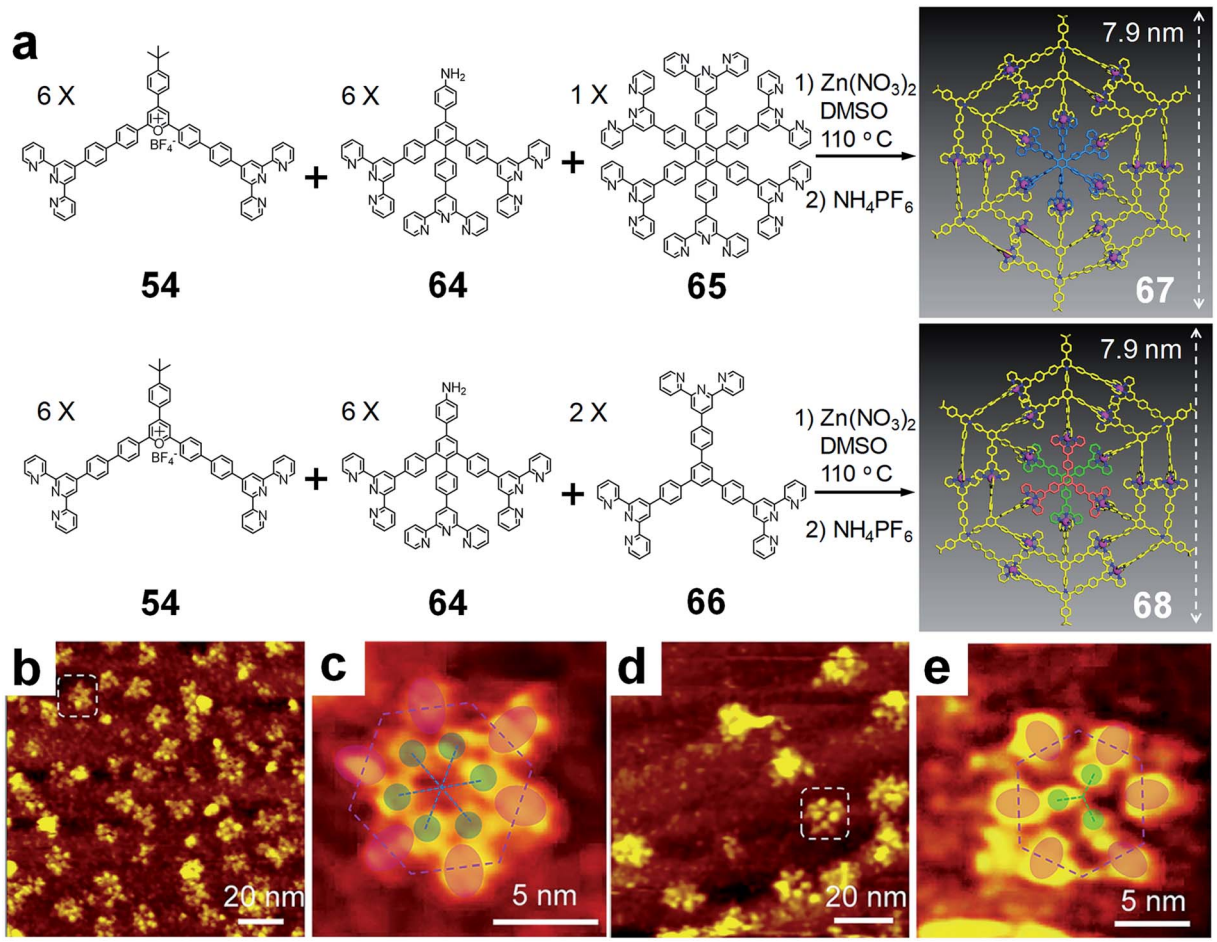

Fig. 14 Metallo-supramolecular spiderwebs by one-pot synthesis/self-assembly strategy. (a) Synthesis and self-assembly of Spiderwebs (b) UHV-LT-STM image of individual **67** on Ag(111) surface; (c) enlarged STM image of one **67** metallo-supramolecule in (b); (d) STM image of individual **68** on Ag(111) surface; (e) zoomed-in STM image of one **68** metallo-supramolecule in (d). Adapted with permission from ref. 29.

in **67** were observed (Fig. 14c and e), which also matched with the structure of the central subunits.

It is worth noting that the multicomponent self-assembly, such as self-sorting by heterotopic ligands and metals,[166,167] subcomponent self-assembly with different reversible bonds,[145,168,169] and template-driven synthesis[170–174] has been extensively used to construct supramolecular architectures. However, all of these strategies rely on non-covalent (coordination) and/or dynamic covalent chemistry. Such a new strategy based on irreversible condensation and dynamic coordination provided an alternative approach to improve the synthetic efficiency in constructing sophisticated metallo-supramolecules with multiple components.

6.4 Hexagonal prism: 3D architecture based on pyrylium salt chemistry

Beyond the synthesis of 2D metallo-supramolecules, pyrylium salt chemistry was also applied in the construction of 3D architectures. For instance, 3D hexagonal prisms **73a**/**b** were achieved by using pentatopic tpy ligands **72a**/**b** through coordination-driven self-assembly with Cd(II),[175] respectively. In the preparation of **72a**/**b**, tritopic pyrylium salt precursors **71a**/**b** were synthesized for further condensation with primary amine precursor **51**. Since the double-layered Kandinsky circles were proved to be robust and thermodynamically stable,[28,160] the introduction of the fifth arm unlikely affected the formation of the concentric hexagon. Indeed, the ESI-MS spectrum proved that the double-layered Kandinsky circle with six free tpy units was the main intermediate during the self-assembly process. As such, this concentric hexagon not only served as the base surface, but also acted as the template of the final hexagonal prism. Furthermore, the STM study showed that the hexagonal prisms had strong tendency to form tubular-like nanostructures (Fig. 15b and c). Due to their high positively charged structures, these metallo-supramolecules exhibited stronger electrostatic interaction with the negatively charged surfaces of the Gram-positive bacteria, leading to a good antimicrobial selectivity toward *S. aureus* and *B. subtilis* (Fig. 15d).

More importantly, different from the conventional construction of prisms by using highly symmetric building blocks, this work utilized an asymmetrical ligand as the building block and the intermediary metallo-macrocycle as the template to construct a 3D metallo-supramolecule. It is anticipated that this new strategy could substantially advance the design and synthesis of 3D metallo-supramolecules by constructing 2D structures as the face for further assembly of 3D architectures with higher complexity.

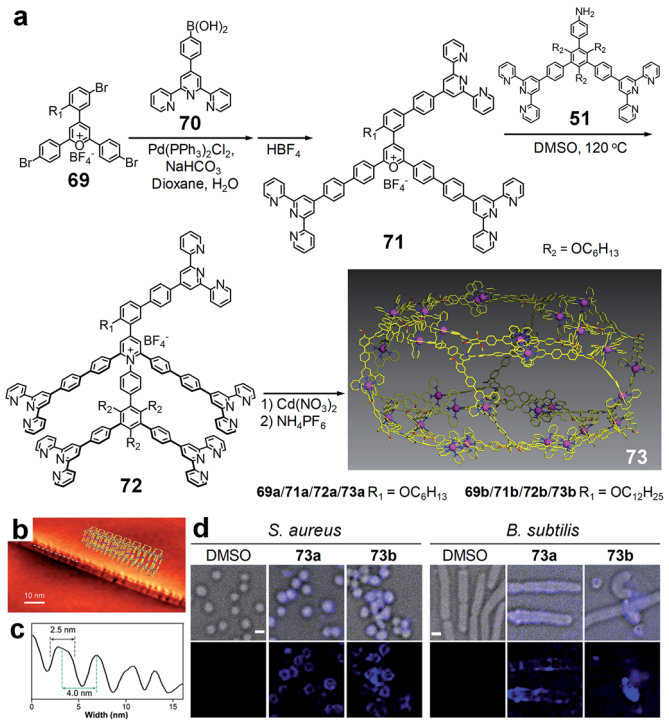

Fig. 15 Metallo-supramolecular hexagonal prism. (a) Synthesis and self-assembly of the hexagonal prism; (b) STM images of the tubular-like nanostructure on the HOPG surface; (c) cross-section of the line marked on the nanostructure shown in panel (b) and (d) 3D deconvolution fluorescence microscopy images of bacterial cells with and without treatment of **73a**/**73b** (4 μmol L^{-1}, DMSO as the control agent). Scale bar: 1 μm. Adapted with permission from ref. 175.

6.5 Functionalization of the concentric hexagon

Benefitting from the rigid backbone and firm scaffold, the structure of the concentric hexagon can be used as a perfect foundation for carrying functional groups at different positions for further functions and applications. Very recently, Li and co-workers have decorated such concentric hexagons with Pt(II) motifs to activate the aggregation-induced phosphorescent emission (AIPE) feature,[176–179] a variant of aggregation-induced emission (AIE), of the metallo-supramolecule.[180] In order to introduce a functional group with fixed orientation, terminal alkyne groups were installed on the external corners of the structure. The introduction of the Pt motif was achieved by Pt–alkyne bond with high stability. With the Pt(II) motifs installed, this 10 nm metallo-supramolecule **77** displayed phosphorescent emission with a lifetime of 218 ns at room temperature. Moreover, benefiting from the synergistic combination of AIE features from the Cd(II)-tpy units on the scaffold and the AIPE from the functional Pt(II) motifs, the self-assembled metallo-supramolecule exhibited significantly enhanced AIPE effect (Fig. 16d).

In this work, the introduction of terminal alkyne groups greatly facilitated the functionalization of supramolecules. The reactive diversity of alkyne groups can be further used to modify the metallo-supramolecules with a variety of functional groups through efficient reactions, such as 'Click Chemistry'. Furthermore, it is worth noting that the introduction of functional groups to such a giant metallo-supramolecular system expanded the scope of discrete functional materials into the dimension beyond 10 nm with molecular level precision.

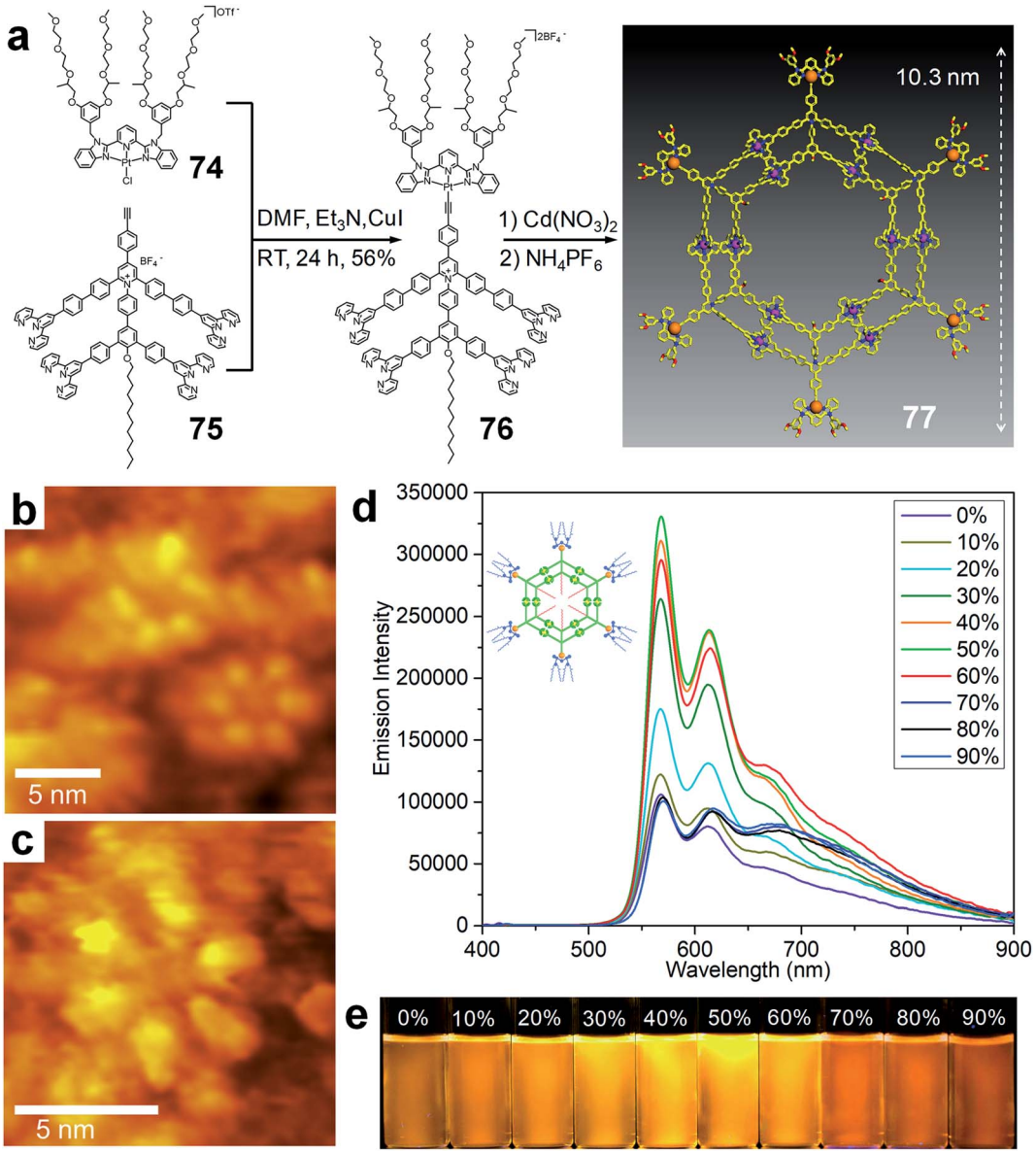

Fig. 16 Functionalized concentric hexagon. (a) Synthesis and self-assembly of functionalized concentric hexagon; (b) STM image of **77** showing the presence of two metallo-supramolecules; (c) enlarged STM image of a single metallo-supramolecule; (d) phosphorescent emission spectra of **77** with N_2 deoxygenated acetonitrile/water solvent; (e) emission photographs of **77** in N_2 deoxygenated acetonitrile/water with various water fractions. Adapted with permission from ref. 180.

7. Conclusion

Since its discovery over one century ago, pyrylium salt chemistry has been mainly limited to the preparation of small molecules and polymers, rather than discrete macrocycles and metallo-supramolecules. The prosperous development of pyrylium salts in the synthesis of small heterocycles and polymers was attributed to the following aspects. First, benefiting from the high reactivity of pyrylium salts, small heterocycles and pyridinium polymers could be easily obtained with a one-step reaction. However, the synthesis of macrocycles and metallo-supramolecules usually involved elaborate design and multiple-step synthesis. Second, the separation of small heterocycles from their staring materials and byproducts is readily approached through simple purification, such as precipitation and chromatography. In contrast, the purification of pyrylium salt-based polymers was mainly realized by precipitation and washing. In comparison, the purification of macrocycles was quite challenging in the presence of reagents and byproducts with similar structures in the earlier years. In addition, many charged metallo-supramolecules with dynamic coordination bonds were unable to stand column separation. Third, most of the heterocycles obtained from pyrylium salt chemistry possessed low molecular weights and simple structures, which could be easily characterized by NMR, MS, and single-crystal X-ray diffraction. However, in front of the

macrocycles and metallo-supramolecules with giant sizes and complex structure, conventional characterization techniques were only able to provide very limited structural information. Therefore, pyrylium salt chemistry was underappreciated in constructing discrete architectures.

With the development of synthetic methods and characterization techniques, the design and synthesis of macrocycles and metallo-supramolecules based on pyrylium salt chemistry have made profound progress in terms of the size, diversity, complexity and functionality in the past two decades. Among them, most of pyrylium salt chemistry was concentrated on the condensation between pyrylium salts and phenylacetate or primary amine precursors. The formal condensation reaction was limited to very few simple phenylacetate analogs and suffered from low efficiency and yield. Unfortunately, no attempts were made to expand the scope of phenylacetate analogs regarding diversity and complexity. Therefore, optimizing the reaction to develop more efficient condensation conditions is expected to advance the future study. In contrast, the latter condensation was applied for a variety of precursors with primary amine. Three strategies, *i.e.*, condensation followed by coupling reaction on pyridinium salts, coupling reaction on pyrylium salts followed by condensation (modular synthetic strategy), and one-pot synthesis/self-assembly, were developed to prepare multitopic building blocks for assembling a series of 2D and 3D metallo-supramolecules with increasing complexity. However, the purification of multitopic pyridinium building blocks with multiple charges and the stability of pyridinium salts under basic condition are the major issues for receiving more broad attention in macrocyclic and metallo-supramolecular chemistry. With the assistance of advanced chromatography techniques, the purification could be solved accordingly.

Beyond the condensation reaction with phenylacetate or primary amine, pyrylium salts on the backbones could also be easily transformed into other functional groups. For instance, the pyridine ring can be achieved by reacting ammonia gas with pyrylium salts without modifying the structures.[114] Using this strategy, other nucleophiles are able to convert the pyrylium ring into a series of heterocycles such as pyridines,[34] phosphinines,[35–37] pyridinium salts,[38,39] thiopyrylium salts[40] and betaine dyes,[41,42] in order to introduce a variety of functions and applications. Moreover, the stability of constructed architectures with arenes or pyridinium salts as backbones can be further enhanced by forming fused conjugated systems to substantially change the electronic and optical properties.[112,181,182]

In addition to modifying the backbones of macrocycles and metallo-supramolecules directly, the functionalities can be introduced by attaching functional groups onto the structures as accessories. For instance, besides the employment of the Pt(II) motif for AIPE property, other luminophores could be attached for tuning the luminescence of the macrocycles and metallo-supramolecules, such as tetraphenylethylene (TPE),[183–187] boron-dipyrromethene (BODIPY),[188–191] triphenylamine,[192,193] pyrene,[194] and perylene diimide. Moreover, the bioactivity of pyrylium salt- and pyridinium salt-based metallo-supramolecules can be further combined with the Ru(II) or Pt(II)-containing functional groups for further application, such as antibacterial materials, anticancer drugs[195,196] and phototherapy agents.[197–199] With precisely-controlled sizes and structures, these large but discrete architectures have emerged as the ideal platforms for installing functional groups to develop novel functional materials by filling the gap between small molecules and polymers. In addition, the employment of pyrylium salt chemistry is expected to advance the design, and simplify the construction and functionalization process.

Through this review, we hope that the research communities in the fields of organic synthesis, metallo-supramolecular chemistry and macrocyclic chemistry are willing to rethink and revisit pyrylium salt chemistry to further advance the synthetic methodology after it was discovered over a century ago. Once the synthetic chemistry is advanced, we should be able to push the limits of macrocyclic and metallo-supramolecular chemistry by creating functional (supra)molecules with increasing complexity, molecular level precision and desired function.

Conflicts of interest

There are no conflicts to declare.

Acknowledgements

The authors acknowledge the support from Shenzhen University and Tencent Founders Alumni Foundation.

References

1 J. J. Koh, C. I. Lee, M. A. Ciulei, H. Han, P. K. Bhowmik, V. Kartazaev and S. K. Gayen, *J. Mol. Struct.*, 2018, **1171**, 458–465.
2 I. K. Sideri, E. Voutyritsa and C. G. Kokotos, *Org. Biomol. Chem.*, 2018, **16**, 4596–4614.
3 M. A. Miranda and H. Garcia, *Chem. Rev.*, 1994, **94**, 1063–1089.
4 E. L. Clennan, C. Liao and E. Ayokosok, *J. Am. Chem. Soc.*, 2008, **130**, 7552–7553.
5 E. L. Clennan and A. K. S. Warrier, *Org. Lett.*, 2009, **11**, 685–688.
6 M. Kamata, J. Hagiwara, T. Hokari, C. Suzuki, R. Fujino, S. Kobayashi, H. S. Kim and Y. Wataya, *Res. Chem. Intermed.*, 2013, **39**, 127–137.
7 A. Baeyer and J. Piccard, *Eur. J. Org. Chem.*, 1911, **384**, 208–224.
8 A. T. Balaban, V. E. Sahini and E. Keplinger, *Tetrahedron*, 1960, **9**, 163–174.
9 P. F. Praill and A. L. Whitear, *J. Chem. Soc.*, 1961, 3573–3579.
10 A. T. Balaban, *Tetrahedron*, 1968, **24**, 5059–5065.
11 A. R. Katritzky, R. D. Tarr, S. M. Heilmann, J. K. Rasmussen and L. R. Krepski, *J. Polym. Sci., Part A: Polym. Chem.*, 1988, **26**, 3323–3336.
12 F. W. Harris, K. C. Chuang, S. A. X. Huang, J. J. Janimak and S. Z. D. Cheng, *Polymer*, 1994, **35**, 4940–4948.

13 R. Jose, D. Truong, H. Han and P. K. Bhowmik, *J. Polym. Res.*, 2015, **22**, 14.
14 P. K. Bhowmik, H. Han, J. J. Cebe, I. K. Nedeltchev, S.-W. Kang and S. Kumar, *Macromolecules*, 2004, **8**, 2688.
15 H. Akahoshi, S. Toshima and K. Itaya, *Am. J. Phys. Chem.*, 1981, **85**, 818–822.
16 P. K. Bhowmik, R. A. Burchett, H. Han and J. J. Cebe, *Macromolecules*, 2001, **39**, 2710–2715.
17 M. S. Simon and P. T. Moore, *J. Polym. Sci., Part A: Polym. Chem.*, 1975, **13**, 1–16.
18 J. S. Moore and S. I. Stupp, *Macromolecules*, 1986, **19**, 1815–1824.
19 P. K. Bhowmik, A. H. Molla, H. Han, M. E. Gangoda and R. N. Bose, *Macromolecules*, 1998, **31**, 621–630.
20 H. Han and P. K. Bhowmik, *Trends Polym. Sci.*, 1995, **3**, 199–206.
21 F. Han, Y. Lu, Q. Zhang, J. Sun, X. Zeng and C. Li, *J. Mater. Chem.*, 2012, **22**, 4106–4112.
22 J. Sun, Y. Lu, L. Wang, D. Cheng, Y. Sun and X. Zeng, *Polym. Chem.*, 2013, **4**, 4045–4051.
23 A. T. Balaban, A. Dinculescu, G. N. Dorofeenko, G. W. Fischer, A. V. Koblik, V. V. Mezheritskii and W. Schroth, *Adv. Heterocycl. Chem.*, 1982, **2**, 85–158.
24 S. Höger, *Pure Appl. Chem.*, 2010, **82**, 821–830.
25 Y. Liu, A. Narita, J. Teyssandier, M. Wagner, S. De Feyter, X. Feng and K. Müllen, *J. Am. Chem. Soc.*, 2016, **138**, 15539–15542.
26 B. Dumslaff, M. Wagner, D. Schollmeyer, A. Narita and K. Müllen, *Chem.–Eur. J.*, 2018, **24**, 11908–11910.
27 M. Wang, K. Wang, C. Wang, M. Huang, X.-Q. Hao, M.-Z. Shen, G.-Q. Shi, Z. Zhang, B. Song, A. Cisneros, M.-P. Song, B. Xu and X. Li, *J. Am. Chem. Soc.*, 2016, **138**, 9258–9268.
28 H. Wang, X. Qian, K. Wang, M. Su, W. W. Haoyang, X. Jiang, R. Brzozowski, M. Wang, X. Gao, Y. Li, B. Xu, P. Eswara, X. Q. Hao, W. Gong, J. L. Hou, J. Cai and X. Li, *Nat. Commun.*, 2018, **9**, 1815.
29 H. Wang, Y. Li, H. Yu, B. Song, S. Lu, X. Q. Hao, Y. Zhang, M. Wang, S. W. Hla and X. Li, *J. Am. Chem. Soc.*, 2019, **141**, 13187–13195.
30 A. T. Balaban, *Org. Synth.*, 1969, **49**, 121.
31 G. N. Dorofeenko and L. B. Olekhnovich, *Chem. Heterocycl. Compd.*, 1972, **8**, 800–802.
32 A. M. Bello and L. P. Kotra, *Tetrahedron Lett.*, 2003, **44**, 9271–9274.
33 A. Moghimi, M. F. Rastegar, M. Ghandi, M. Taghizadeh, A. Yari, M. Shamsipur, G. P. A. Yap and H. Rahbarnoohi, *J. Org. Chem.*, 2002, **67**, 2065–2074.
34 Y. Liu, M. Han, H.-Y. Zhang, L.-X. Yang and W. Jiang, *Org. Lett.*, 2008, **10**, 2873–2876.
35 C. Muller and D. Vogt, *Dalton Trans.*, 2007, 5505–5523.
36 P. Tokarz and P. M. Zagorski, *Chem. Heterocycl. Compd.*, 2017, **53**, 858–860.
37 N. Nagahora, T. Ogawa, M. Honda, M. Fujii, H. Tokumaru, T. Sasamori, K. Shioji and K. Okuma, *Chem. Lett.*, 2015, **44**, 706–708.
38 J. Fortage, C. Peltier, F. Nastasi, F. Puntoriero, F. Tuyeras, S. Griveau, F. Bedioui, C. Adamo, I. Ciofini, S. Campagna and P. P. Laine, *J. Am. Chem. Soc.*, 2010, **132**, 16700–16713.
39 J. Fortage, C. Peltier, C. Perruchot, Y. Takemoto, Y. Teki, F. Bedioui, V. Marvaud, G. Dupeyre, L. Pospisil, C. Adamo, M. Hromadova, I. Ciofini and P. P. Laine, *J. Am. Chem. Soc.*, 2012, **134**, 2691–2705.
40 T. Abalos, D. Jimenez, M. Moragues, S. Royo, R. Martinez-Manez, F. Sancenon, J. Soto, A. M. Costero, M. Parra and S. Gil, *Dalton Trans.*, 2010, **39**, 3449–3459.
41 C. Reichardt, D. Che, G. Heckenkemper and G. Schäfer, *Eur. J. Org. Chem.*, 2001, **2001**, 2343–2361.
42 C. Reichardt, *Pure Appl. Chem.*, 2004, **76**, 1903–1919.
43 C. H. Basch, J. Liao, J. Xu, J. J. Piane and M. P. Watson, *J. Am. Chem. Soc.*, 2017, **139**, 5313–5316.
44 J. Wu, P. S. Grant, X. Li, A. Noble and V. K. Aggarwal, *Angew. Chem., Int. Ed.*, 2019, **58**, 5697–5701.
45 X. H. Cheng, S. Höger and D. Fenske, *Org. Lett.*, 2003, **5**, 2587–2589.
46 F. Ba, F. R. L. Guen, N. Cabon, P. Le Poul, S. Golhen, N. Le Poul and B. Caro, *J. Organomet. Chem.*, 2010, **695**, 235–243.
47 S. Arava and C. E. Diesendruck, *Synthesis*, 2017, **49**, 3535–3545.
48 I. Y. Kargapolova, K. S. Shmuilovich, I. V. Beregovaya and N. A. Orlova, *Russ. Chem. Bull.*, 2010, **59**, 1414.
49 J. Wu, L. He, A. Noble and V. K. Aggarwal, *J. Am. Chem. Soc.*, 2018, **140**, 10700–10704.
50 B. Breit, R. Winde, T. Mackewitz, R. Paciello and K. Harms, *Chem.–Eur. J.*, 2001, **7**, 3106–3121.
51 R. Perez-Ruiz, M. C. Jimenez and M. A. Miranda, *Acc. Chem. Res.*, 2014, **47**, 1359–1368.
52 O. Dangles and J. A. Fenger, *Molecules*, 2018, **23**, 1970.
53 E. A. Zvezdina, M. P. Zhdanova and G. N. Dorofeenko, *Russ. Chem. Rev.*, 1982, **51**, 469–484.
54 Q. Michaudel, T. Chauvire, V. Kottisch, M. J. Supej, K. J. Stawiasz, L. X. Shen, W. R. Zipfel, H. D. Abruna, J. H. Freed and B. P. Fors, *J. Am. Chem. Soc.*, 2017, **139**, 15530–15538.
55 L. M. M. Pascual, D. G. Dunford, A. E. Goetz, K. A. Ogawa and A. J. Boydston, *Synlett*, 2016, **27**, 759–762.
56 J. A. Mikroyannidis, *Polymer*, 2000, **41**, 8193–8204.
57 J. A. Mikroyannidis, *Macromolecules*, 2002, **35**, 9289–9295.
58 I. K. Spiliopoulos and J. A. Mikroyannidis, *Macromolecules*, 1998, **31**, 1236–1245.
59 I. K. Spiliopoulos and J. A. Mikroyannidis, *Macromolecules*, 2002, **35**, 7254–7261.
60 I. K. Spiliopoulos and J. A. Mikroyannidis, *Macromolecules*, 2002, **35**, 2149–2156.
61 J. A. Mikroyannidis, *Chem. Mater.*, 2003, **15**, 1865–1871.
62 A. Gomez-Valdemoro, R. Martinez-Manez, F. Sancenon, F. C. Garcia and J. M. Garcia, *Macromolecules*, 2010, **43**, 7111–7121.
63 F. Garcia, J. M. Garcia, B. Garcia-Acosta, R. Martinez-Manez, F. Sancenon and J. Soto, *Chem. Commun.*, 2005, 2790–2792.
64 B. Garcia-Acosta, M. Comes, J. L. Bricks, M. A. Kudinova, V. V. Kurdyukov, A. I. Tolmachev, A. B. Descalzo, M. D. Marcos, R. Martinez-Manez, A. Moreno,

F. Sancenon, J. Soto, L. A. Villaescusa, K. Rurack, J. M. Barat, I. Escriche and P. Amoros, *Chem. Commun.*, 2006, 2239–2241.
65 B. Garcia-Acosta, F. Garcia, J. M. Garcia, R. Martinez-Manez, F. Sancenon, N. San-Jose and J. Soto, *Org. Lett.*, 2007, **9**, 2429–2432.
66 S. E. Bustamante Fonseca, B. L. Rivas, J. M. García Pérez, S. Vallejos Calzada and F. García, *J. Appl. Polym. Sci.*, 2018, **135**, 46185.
67 K. Novak, V. Enkelmann, G. Wegner and K. B. Wagener, *Angew. Chem., Int. Ed.*, 1993, **32**, 1614–1616.
68 R. Z. Lange, G. Hofer, T. Weber and A. D. Schlüter, *J. Am. Chem. Soc.*, 2017, **139**, 2053–2059.
69 R. Z. Lange, K. Synnatschke, H. Y. Qi, N. Huber, G. Hofer, B. K. Liang, C. Huck, A. Pucci, U. Kaiser, C. Backes and A. D. Schluter, *Angew. Chem., Int. Ed.*, 2020, **59**, 5683–5695.
70 G. Wenz, *Angew. Chem., Int. Ed.*, 1994, **33**, 803–822.
71 E. M. M. Del Valle, *Process Biochem.*, 2004, **39**, 1033–1046.
72 R. Bonnett, *Chem. Soc. Rev.*, 1995, **24**, 19–33.
73 M. Ethirajan, Y. Chen, P. Joshi and R. K. Pandey, *Chem. Soc. Rev.*, 2011, **40**, 340–362.
74 L.-L. Li and E. W.-G. Diau, *Chem. Soc. Rev.*, 2013, **42**, 291–304.
75 R. M. Izatt, J. S. Bradshaw, S. A. Nielsen, J. D. Lamb, J. J. Christensen and D. Sen, *Chem. Rev.*, 1985, **85**, 271–339.
76 R. M. Izatt, K. Pawlak, J. S. Bradshaw and R. L. Bruening, *Chem. Rev.*, 1991, **91**, 1721–2085.
77 V. Böhmer, *Angew. Chem., Int. Ed.*, 1995, **34**, 713–745.
78 G. Ghale and W. M. Nau, *Acc. Chem. Res.*, 2014, **47**, 2150–2159.
79 M. Xue, Y. Yang, X. Chi, Z. Zhang and F. Huang, *Acc. Chem. Res.*, 2012, **45**, 1294–1308.
80 H. Zhang, Z. Liu and Y. Zhao, *Chem. Soc. Rev.*, 2018, **47**, 5491–5528.
81 M. Iyoda and H. Shimizu, *Chem. Soc. Rev.*, 2015, **44**, 6411–6424.
82 D. Eisenberg, R. Shenhar and M. Rabinovitz, *Chem. Soc. Rev.*, 2010, **39**, 2879–2890.
83 S. Lee, C.-H. Chen and A. H. Flood, *Nat. Chem.*, 2013, **5**, 704–710.
84 V. Balzani, A. Credi, F. M. Raymo and J. F. Stoddart, *Angew. Chem., Int. Ed.*, 2000, **39**, 3348–3391.
85 E. R. Kay, D. A. Leigh and F. Zerbetto, *Angew. Chem., Int. Ed.*, 2007, **46**, 72–191.
86 E. M. Driggers, S. P. Hale, J. Lee and N. K. Terrett, *Nat. Rev. Drug Discovery*, 2008, **7**, 608–624.
87 F. Sansone and A. Casnati, *Chem. Soc. Rev.*, 2013, **42**, 4623–4639.
88 L. Pu, *Chem. Rev.*, 1998, **98**, 2405–2494.
89 K. I. Assaf and W. M. Nau, *Chem. Soc. Rev.*, 2015, **44**, 394–418.
90 J. Cai and J. L. Sessler, *Chem. Soc. Rev.*, 2014, **43**, 6198–6213.
91 Q. He, G. I. Vargas-Zúñiga, S. H. Kim, S. K. Kim and J. L. Sessler, *Chem. Rev.*, 2019, **119**, 9753–9835.
92 Y. Ding, Y. Tang, W. Zhu and Y. Xie, *Chem. Soc. Rev.*, 2015, **44**, 1101–1112.
93 Y. Ding, W.-H. Zhu and Y. Xie, *Chem. Rev.*, 2017, **117**, 2203–2256.
94 W. Zhang and J. S. Moore, *Angew. Chem., Int. Ed.*, 2006, **45**, 4416–4439.
95 S. Höger, *Chem.–Eur. J.*, 2004, **10**, 1320–1329.
96 D. Zhao and J. S. Moore, *Chem. Commun.*, 2003, 807–818.
97 C. Grave and A. D. Schlüter, *Eur. J. Org. Chem.*, 2002, **2002**, 3075–3098.
98 P.-H. Ge, W. Fu, W. A. Herrmann, E. Herdtweck, C. Campana, R. D. Adams and U. H. F. Bunz, *Angew. Chem., Int. Ed.*, 2000, **112**, 3753.
99 H. A. Staab and K. Neunhoeffer, *Synthesis*, 1974, 424.
100 D. Lin, Y. Wei, A. Peng, H. Zhang, C. Zhong, D. Lu, H. Zhang, X. Zheng, L. Yang, Q. Feng, L. Xie and W. Huang, *Nat. Commun.*, 2020, **11**, 1756.
101 Y. Yu, L. Bian, Y. Zhang, Z. Liu, Y. Li, R. Zhang, R. Ju, C. Yin, L. Yang, M. Yi, L. Xie and W. Huang, *ACS Omega*, 2019, **4**, 5863–5869.
102 Y. Wei, Q. Feng, H. Liu, X. Wang, D. Lin, S. Xie, M. Yi, L.-H. Xie and W. Huang, *Eur. J. Org. Chem.*, 2018, **2018**, 7009–7016.
103 G. Zhang, Y. Wei, J. Wang, Y. Liu, L. Xie, L. Wang, B. Ren and W. Huang, *Mater. Chem. Front.*, 2017, **1**, 455–459.
104 L. Wang, G.-W. Zhang, C.-J. Ou, L.-H. Xie, J.-Y. Lin, Y.-Y. Liu and W. Huang, *Org. Lett.*, 2014, **16**, 1748–1751.
105 J. S. Moore and J. Zhang, *Angew. Chem., Int. Ed.*, 1992, **31**, 922–924.
106 J. Zhang, D. J. Pesak, J. L. Ludwick and J. S. Moore, *J. Am. Chem. Soc.*, 1994, **116**, 4227–4239.
107 S. Sun, C. Ou, D. Lin, Z. Zuo, Y. Yan, Y. Wei, Y. Liu, L. Xie and W. Huang, *Tetrahedron*, 2018, **74**, 5833–5838.
108 S. Höger, A.-D. Meckenstock and S. Müller, *Chem.–Eur. J.*, 1998, **4**, 2423–2434.
109 S. Höger, S. Rosselli, A. D. Ramminger and V. Enkelmann, *Org. Lett.*, 2002, **4**, 4269–4272.
110 T. S. Balaban and A. T. Balaban, *Sci. Synth.*, 2003, 11–200.
111 S. Klyatskaya, N. Dingenouts, C. Rosenauer, B. Muller and S. Höger, *J. Am. Chem. Soc.*, 2006, **128**, 3150–3151.
112 X. H. Cheng, A. V. Heyen, W. Mamdouh, H. Uji-i, F. De Schryver, S. Höger and S. De Feyter, *Langmuir*, 2007, **23**, 1281–1286.
113 K. Becker, M. Fritzsche, S. Höger and J. M. Lupton, *J. Phys. Chem. B*, 2008, **112**, 4849–4853.
114 N. Shabelina, S. Klyatskaya, V. Enkelmann and S. Höger, *C. R. Chim.*, 2009, **12**, 430–436.
115 T. Kudernac, N. Shabelina, W. Mamdouh, S. Höger and S. De Feyter, *Beilstein J. Nanotechnol.*, 2011, **2**, 674–680.
116 C. Allolio, T. Stangl, T. Eder, D. Schmitz, J. Vogelsang, S. Höger, D. Horinek and J. M. Lupton, *J. Phys. Chem. B*, 2018, **122**, 6431–6441.
117 S. Höger, A. D. Meckenstock and H. Pellen, *J. Org. Chem.*, 1997, **62**, 4556–4557.
118 S. Rosselli, A.-D. Ramminger, T. Wagner, B. Silier, S. Wiegand, W. Häußler, G. Lieser, V. Scheumann and S. Höger, *Angew. Chem., Int. Ed.*, 2001, **40**, 3137–3141.
119 Y. Tobe, K. Tahara and S. De Feyter, *Bull. Chem. Soc. Jpn.*, 2016, **89**, 1277–1306.

120 K. Becker, P. G. Lagoudakis, G. Gaefke, S. Höger and J. M. Lupton, *Angew. Chem., Int. Ed.*, 2007, **46**, 3450–3455.
121 K. Becker, G. Gaefke, J. Rolffs, S. Höger and J. M. Lupton, *Chem. Commun.*, 2010, 4686–4688.
122 C. Schweez, P. Shushkov, S. Grimme and S. Höger, *Angew. Chem., Int. Ed.*, 2016, **55**, 3328–3333.
123 C. Schweez and S. Höger, *Chem.–Eur. J.*, 2018, **24**, 12006–12009.
124 G. Ohlendorf, C. W. Mahler, S.-S. Jester, G. Schnakenburg, S. Grimme and S. Höger, *Angew. Chem., Int. Ed.*, 2013, **52**, 12086–12090.
125 B. Dumslaff, A. N. Reuss, M. Wagner, X. Feng, A. Narita, G. Fytas and K. Müllen, *Angew. Chem., Int. Ed.*, 2017, **56**, 10602–10606.
126 D. Mossinger, J. Hornung, S. Lei, S. De Feyter and S. Höger, *Angew. Chem., Int. Ed.*, 2007, **46**, 6802–6806.
127 K. Tahara, S. Lei, D. Mossinger, H. Kozuma, K. Inukai, M. Van der Auweraer, F. C. De Schryver, S. Höger, Y. Tobe and S. De Feyter, *Chem. Commun.*, 2008, 3897–3899.
128 S. Lei, A. Ver Heyen, S. De Feyter, M. Surin, R. Lazzaroni, S. Rosenfeldt, M. Ballauff, P. Lindner, D. Mossinger and S. Höger, *Chem.–Eur. J.*, 2009, **15**, 2518–2535.
129 D. Mossinger, D. Chaudhuri, T. Kudernac, S. Lei, S. De Feyter, J. M. Lupton and S. Höger, *J. Am. Chem. Soc.*, 2010, **132**, 1410–1423.
130 R. May, S. S. Jester and S. Höger, *J. Am. Chem. Soc.*, 2014, **136**, 16732–16735.
131 D. Wursch, R. May, G. Wiederer, S. S. Jester, S. Höger, J. Vogelsang and J. M. Lupton, *Chem. Commun.*, 2017, 352–355.
132 A. Idelson, C. Sterzenbach, S.-S. Jester, C. Tschierske, U. Baumeister and S. Höger, *J. Am. Chem. Soc.*, 2017, **139**, 4429–4434.
133 M. Fujita, J. Yazaki and K. Ogura, *J. Am. Chem. Soc.*, 1990, **112**, 5645–5647.
134 B. Olenyuk, J. A. Whiteford, A. Fechtenkötter and P. J. Stang, *Nature*, 1999, **398**, 796–799.
135 Q.-F. Sun, J. Iwasa, D. Ogawa, Y. Ishido, S. Sato, T. Ozeki, Y. Sei, K. Yamaguchi and M. Fujita, *Science*, 2010, **328**, 1144–1147.
136 G. R. Newkome, P. Wang, C. N. Moorefield, T. J. Cho, P. P. Mohapatra, S. Li, S.-H. Hwang, O. Lukoyanova, L. Echegoyen, J. A. Palagallo, V. Iancu and S.-W. Hla, *Science*, 2006, **312**, 1782–1785.
137 K. S. Chichak, S. J. Cantrill, A. R. Pease, S.-H. Chiu, G. W. V. Cave, J. L. Atwood and J. F. Stoddart, *Science*, 2004, **304**, 1308–1312.
138 I. A. Riddell, M. M. J. Smulders, J. K. Clegg, Y. R. Hristova, B. Breiner, J. D. Thoburn and J. R. Nitschke, *Nat. Chem.*, 2012, **4**, 751–756.
139 J.-F. Ayme, J. E. Beves, D. A. Leigh, R. T. McBurney, K. Rissanen and D. Schultz, *Nat. Chem.*, 2012, **4**, 15–20.
140 E. C. Constable, *Chem. Soc. Rev.*, 2007, **36**, 246–253.
141 T. R. Cook, Y.-R. Zheng and P. J. Stang, *Chem. Rev.*, 2013, **113**, 734–777.
142 G.-Y. Wu, L.-J. Chen, L. Xu, X.-L. Zhao and H.-B. Yang, *Coord. Chem. Rev.*, 2018, **369**, 39–75.
143 M. Pan, W.-M. Liao, S.-Y. Yin, S.-S. Sun and C.-Y. Su, *Chem. Rev.*, 2018, **118**, 8889–8935.
144 F. Würthner, C.-C. You and C. R. Saha-Möller, *Chem. Soc. Rev.*, 2004, **33**, 133–146.
145 M. M. J. Smulders, I. A. Riddell, C. Browne and J. R. Nitschke, *Chem. Soc. Rev.*, 2013, **42**, 1728–1754.
146 D. Zhang, T. K. Ronson and J. R. Nitschke, *Acc. Chem. Res.*, 2018, **51**, 2423–2436.
147 M. J. Wiester, P. A. Ulmann and C. A. Mirkin, *Angew. Chem., Int. Ed.*, 2011, **50**, 114–137.
148 L.-J. Chen, H.-B. Yang and M. Shionoya, *Chem. Soc. Rev.*, 2017, **46**, 2555–2576.
149 S. Chakraborty and G. R. Newkome, *Chem. Soc. Rev.*, 2018, **47**, 3991–4016.
150 M. Ruben, J. Rojo, F. J. Romero-Salguero, L. H. Uppadine and J.-M. Lehn, *Angew. Chem., Int. Ed.*, 2004, **43**, 3644–3662.
151 M. Fujita, M. Tominaga, A. Hori and B. Therrien, *Acc. Chem. Res.*, 2005, **38**, 369–378.
152 M. Han, D. M. Engelhard and G. H. Clever, *Chem. Soc. Rev.*, 2014, **43**, 1848–1860.
153 P. Jin, S. J. Dalgarno and J. L. Atwood, *Coord. Chem. Rev.*, 2010, **254**, 1760–1768.
154 Y. T. Chan, X. P. Li, J. Yu, G. A. Carri, C. N. Moorefield, G. R. Newkome and C. Wesdemiotis, *J. Am. Chem. Soc.*, 2011, **133**, 11967–11976.
155 X. P. Li, Y. T. Chan, M. Casiano-Maldonado, J. Yu, G. A. Carri, G. R. Newkome and C. Wesdemiotis, *Anal. Chem.*, 2011, **83**, 6667–6674.
156 M. Fujita, O. Sasaki, T. Mitsuhashi, T. Fujita, J. Yazaki, K. Yamaguchi and K. Ogura, *Chem. Commun.*, 1996, 1535–1536.
157 M. Schweiger, S. R. Seidel, A. M. Arif and P. J. Stang, *Inorg. Chem.*, 2002, **41**, 2556–2559.
158 H. Jiang and W. Lin, *J. Am. Chem. Soc.*, 2003, **125**, 8084–8085.
159 T. Weilandt, R. W. Troff, H. Saxell, K. Rissanen and C. A. Schalley, *Inorg. Chem.*, 2008, **47**, 7588–7598.
160 M. Wang, C. Wang, X.-Q. Hao, J. Liu, X. Li, C. Xu, A. Lopez, L. Sun, M.-P. Song, H.-B. Yang and X. Li, *J. Am. Chem. Soc.*, 2014, **136**, 6664–6671.
161 B. Sun, M. Wang, Z. Lou, M. Huang, C. Xu, X. Li, L.-J. Chen, Y. Yu, G. L. Davis, B. Xu, H.-B. Yang and X. Li, *J. Am. Chem. Soc.*, 2015, **137**, 1556–1564.
162 B. Song, Z. Zhang, K. Wang, C.-H. Hsu, O. Bolarinwa, J. Wang, Y. Li, G.-Q. Yin, E. Rivera, H.-B. Yang, C. Liu, B. Xu and X. Li, *Angew. Chem., Int. Ed.*, 2017, **56**, 5258–5262.
163 G.-Q. Yin, H. Wang, X.-Q. Wang, B. Song, L.-J. Chen, L. Wang, X.-Q. Hao, H.-B. Yang and X. Li, *Nat. Commun.*, 2018, **9**, 567.
164 L. Wang, B. Song, S. Khalife, Y. Li, L.-J. Ming, S. Bai, Y. Xu, H. Yu, M. Wang, H. Wang and X. Li, *J. Am. Chem. Soc.*, 2020, **142**, 1811–1821.
165 Y. T. Chan, X. P. Li, C. N. Moorefield, C. Wesdemiotis and G. R. Newkome, *Chem.–Eur. J.*, 2011, **17**, 7750–7754.
166 S. Leininger, B. Olenyuk and P. J. Stang, *Chem. Rev.*, 2000, **100**, 853–908.

167 R. Chakrabarty, P. S. Mukherjee and P. J. Stang, *Chem. Rev.*, 2011, **111**, 6810–6918.
168 A. M. Castilla, W. J. Ramsay and J. R. Nitschke, *Acc. Chem. Res.*, 2014, **47**, 2063–2073.
169 A. J. McConnell, C. S. Wood, P. P. Neelakandan and J. R. Nitschke, *Chem. Rev.*, 2015, **115**, 7729–7793.
170 X. C. Lu, X. P. Li, Y. Cao, A. Schultz, J. L. Wang, C. N. Moorefield, C. Wesdemiotis, S. Z. D. Cheng and G. R. Newkome, *Angew. Chem., Int. Ed.*, 2013, **52**, 7728–7731.
171 J. L. Wang, X. P. Li, X. C. Lu, I. F. Hsieh, Y. Cao, C. N. Moorefield, C. Wesdemiotis, S. Z. D. Cheng and G. R. Newkome, *J. Am. Chem. Soc.*, 2011, **133**, 11450–11453.
172 Y. Kubota, S. Sakamoto, K. Yamaguchi and M. Fujita, *Proc. Natl. Acad. Sci. U. S. A.*, 2002, **99**, 4854–4856.
173 K. Kumazawa, K. Biradha, T. Kusukawa, T. Okano and M. Fujita, *Angew. Chem., Int. Ed.*, 2003, **42**, 3909–3913.
174 P. S. Bols and H. L. Anderson, *Acc. Chem. Res.*, 2018, **51**, 2083–2092.
175 H. Wang, C. H. Liu, K. Wang, M. Wang, H. Yu, S. Kandapal, R. Brzozowski, B. Xu, M. Wang, S. Lu, X. Q. Hao, P. Eswara, M. P. Nieh, J. Cai and X. Li, *J. Am. Chem. Soc.*, 2019, **141**, 16108–16116.
176 L. Ravotto and P. Ceroni, *Coord. Chem. Rev.*, 2017, **346**, 62–76.
177 Y. You, H. S. Huh, K. S. Kim, S. W. Lee, D. Kim and S. Y. Park, *Chem. Commun.*, 2008, 3998–4000.
178 Q. Zhao, L. Li, F. Li, M. Yu, Z. Liu, T. Yi and C. Huang, *Chem. Commun.*, 2008, 685–687.
179 S. Liu, H. Sun, Y. Ma, S. Ye, X. Liu, X. Zhou, X. Mou, L. Wang, Q. Zhao and W. Huang, *J. Mater. Chem.*, 2012, **22**, 22167–22173.
180 Y. Li, G.-F. Huo, B. Liu, B. Song, Y. Zhang, X. Qian, H. Wang, G.-Q. Yin, A. Filosa, W. Sun, S. W. Hla, H.-B. Yang and X. Li, *J. Am. Chem. Soc.*, 2020, **142**, 14638–14648.
181 D. Wu, L. Zhi, G. J. Bodwell, G. Cui, N. Tsao and K. Müllen, *Angew. Chem., Int. Ed.*, 2007, **46**, 5417–5420.
182 J. Fortage, G. Dupeyre, F. Tuyèras, V. Marvaud, P. Ochsenbein, I. Ciofini, M. Hromadová, L. Pospísil, A. Arrigo, E. Trovato, F. Puntoriero, P. P. Lainé and S. Campagna, *Inorg. Chem.*, 2013, **52**, 11944–11955.
183 X. Yan, H. Wang, C. E. Hauke, T. R. Cook, M. Wang, M. L. Saha, Z. Zhou, M. Zhang, X. Li, F. Huang and P. J. Stang, *J. Am. Chem. Soc.*, 2015, **137**, 15276–15286.
184 X. Yan, T. R. Cook, P. Wang, F. Huang and P. J. Stang, *Nat. Chem.*, 2015, **7**, 342–348.
185 C. Lu, M. Zhang, D. Tang, X. Yan, Z. Zhang, Z. Zhou, B. Song, H. Wang, X. Li, S. Yin, H. Sepehrpour and P. J. Stang, *J. Am. Chem. Soc.*, 2018, **140**, 7674–7680.
186 J. Dong, Y. Pan, H. Wang, K. Yang, L. Liu, Z. Qiao, Y. Di Yuan, S. B. Peh, J. Zhang, L. Shi, H. Liang, Y. Han, X. Li, J. Jiang, B. Liu and D. Zhao, *Angew. Chem., Int. Ed.*, 2019, **59**, 10151–10159.
187 J. Dong, Y. Pan, H. Wang, K. Yang, L. Liu, Z. Qiao, Y. D. Yuan, S. B. Peh, J. Zhang, L. Shi, H. Liang, Y. Han, X. Li, J. Jiang, B. Liu and D. Zhao, *Angew. Chem., Int. Ed.*, 2020, **59**, 10151–10159.
188 M. Zhang, M. L. Saha, M. Wang, Z. Zhou, B. Song, C. Lu, X. Yan, X. Li, F. Huang, S. Yin and P. J. Stang, *J. Am. Chem. Soc.*, 2017, **139**, 5067–5074.
189 A. J. Musser, P. P. Neelakandan, J. M. Richter, H. Mori, R. H. Friend and J. R. Nitschke, *J. Am. Chem. Soc.*, 2017, **139**, 12050–12059.
190 M. Käseborn, J. J. Holstein, G. H. Clever and A. Lützen, *Angew. Chem., Int. Ed.*, 2018, **57**, 12171–12175.
191 J. Zhou, Y. Zhang, G. Yu, M. R. Crawley, C. R. P. Fulong, A. E. Friedman, S. Sengupta, J. Sun, Q. Li, F. Huang and T. R. Cook, *J. Am. Chem. Soc.*, 2018, **140**, 7730–7736.
192 J. Wang, C. He, P. Wu, J. Wang and C. Duan, *J. Am. Chem. Soc.*, 2011, **133**, 12402–12405.
193 J. L. Zhu, L. Xu, Y. Y. Ren, Y. Zhang, X. Liu, G. Q. Yin, B. Sun, X. Cao, Z. Chen, X. L. Zhao, H. Tan, J. Chen, X. Li and H. B. Yang, *Nat. Commun.*, 2019, **10**, 4285.
194 X. Chang, Z. Zhou, C. Shang, G. Wang, Z. Wang, Y. Qi, Z. Y. Li, H. Wang, L. Cao, X. Li, Y. Fang and P. J. Stang, *J. Am. Chem. Soc.*, 2019, **141**, 1757–1765.
195 Y. B. Zhao, L. Q. Zhang, X. Li, Y. H. Shi, R. R. Ding, M. T. Teng, P. Zhang, C. S. Cao and P. J. Stang, *Proc. Natl. Acad. Sci. U. S. A.*, 2019, **116**, 4090–4098.
196 I. V. Grishagin, J. B. Pollock, S. Kushal, T. R. Cook, P. J. Stang and B. Z. Olenyuk, *Proc. Natl. Acad. Sci. U. S. A.*, 2014, **111**, 18448–18453.
197 S. J. Gao, X. Z. Yan, G. C. Xie, M. Zhu, X. Y. Ju, P. J. Stang, Y. Tian and Z. W. Niu, *Proc. Natl. Acad. Sci. U. S. A.*, 2019, **116**, 23437–23443.
198 Y. Sun, F. Ding, Z. X. Zhou, C. L. Li, M. P. Pu, Y. L. Xu, Y. B. Zhan, X. J. Lu, H. B. Li, G. F. Yang, Y. Sun and P. J. Stang, *Proc. Natl. Acad. Sci. U. S. A.*, 2019, **116**, 1968–1973.
199 Z. X. Zhou, J. P. Liu, J. J. Huang, T. W. Rees, Y. L. Wang, H. Wang, X. P. Li, H. Chao and P. J. Stang, *Proc. Natl. Acad. Sci. U. S. A.*, 2019, **116**, 20296–20302.

